IEEE Access
Multidisciplinary : Rapid Review : Open Access Journal

Date of publication xxxx 00, 0000, date of current version xxxx 00, 0000.

Digital Object Identifier 10.1109/ACCESS.2017.DOI

Robust Collaborative Team Formation Control of Hybrid Teams of Biped Robots and Wheeled Vehicles Under External Disturbance and Communication Interactions

BOR-SEN CHEN[1,2], (Life Fellow, IEEE), JUN-HAO LIN[1]
[1]Department of Electrical Engineering, National Tsing Hua University, Hsinchu 30013, Taiwan
[2]Department of Electrical Engineering, Yuan Ze University, Taoyuan 32003, Taiwan

Corresponding author: Bor-Sen Chen (bschen@ee.nthu.edu.tw)

This work was supported by the Ministry of Science and Technology of Taiwan under Grant MOST 108-2221-E-007-099-MY3.

ABSTRACT In this study, a collaborative team formation system of hybrid teams of biped robots and tractor-trailers is designed for some common task. The collaborative team formation system consists of a number of hybrid team formation subsystems. Each hybrid team formation subsystem is composed of a tractor-trailer as the leader and a group of biped robots as followers. For the convenience of collaborative team formation design, novel reference models are proposed to generate the desired collaborative time-varying leader-follower team formation for the cooperative tractor-trailers and biped robots in each hybrid team. Accordingly, the collaborative team formation design problem is simplified to a set of independent robust model reference tracking design problems for each agent under external disturbances and communication couplings from other agents. Subsequently, the robust H_∞ decentralized collaborative team formation tracking control strategy is proposed to achieve the team formation tracking control for each agent and efficiently attenuate the effect of external disturbance and communication coupling from other agents on the decentralized model reference tracking performance of each agent. In order to avoid solving the difficult Hamilton-Jacobi inequality (HJI) of the robust H_∞ decentralized collaborative team formation tracking control for each agent, the numerical linear parameter-varying (LPV) modeling method is employed to approximate the nonlinear team formation tracking error dynamic system of each agent such that the HJI can be equivalently transformed to a set of linear-matrix inequalities (LMIs) which can be efficiently solved by MATLAB LMI TOOLBOX. Since the robust H_∞ decentralized collaborative team formation tracking control scheme is employed based on local information, the collaborative team formation system can be extended to very large-scale biped robots and tractor-trailers. Finally, a simulation example of robust H_∞ decentralized collaborative team formation tracking control design of three collaborative teams with one tractor-trailer as the leader and six biped robots as followers in each hybrid team compared with the optimal H_2 decentralized method is given to verify the effectiveness of the proposed scheme.

INDEX TERMS Collaborative team formation, Hybrid team, decentralized formation control, leader-follower formation, robust H_∞ control, reference model, biped robot, tractor-trailer, linear matrix inequality.

I. INTRODUCTION

WITH the development of wireless communication techniques and the concept of smart city, the applications of autonomous systems have been a hot topic in academic research and industry areas for decades. Especially, for the applications of autonomous mobile robots, they can sense surroundings, design trajectories, and make decisions to accomplish their tasks autonomously, efficiently, and safely [1]. In addition, the various types of locomotion mechanisms could allow these mobile robots to reach more unknown or hazardous environments and to cope with diverse requirements.

So far, biped robots and wheeled robots are the two most representative mobile robots. For biped robots, the legged locomotion mechanism makes them explore complex and uneven terrain to execute dangerous tasks. However, the complex nonlinear system of biped robot makes them inherently difficult being controlled. Therefore, the state-of-art researches in the field of bipedal locomotion focus on two objectives: generate stable periodic gait to realize stable walking and design joint-space controller to track certain desired leg motions, including gait generation [2], [3], zero-moment-point method [4]- [7], and zero-dynamic-based framework [8], [9].

On the other hand, the wheeled robot is the most general and widespread mobile robot in mobile robotics and man-made vehicles due to its simplicity, efficiency, and flexibility. Therefore, there have existed so many researches on the motion task of wheeled robot, such as path following [10], [11] and trajectory tracking [12], [13]. Furthermore, to enhance the transportation capacity and decrease the cost simultaneously, the wheeled robot with a passive trailer called tractor-trailer is also an attracting issue in mobile robot field [14], [15], [16]. However, due to the nonholonomic constraints and passive trailers, the tracking control design problem for tractor-trailer is still complicated and challenging.

Recently, since the missions of mobile robots have become more complicated and hazardous, instead of a powerful single robot, the collaboration among robots can provide more flexibility and robustness in these missions. Moreover, with the technical advances in wireless communication, sensors, and the embedded computing ability [17], the collaborative team formation control problem for multi-agent systems has been a popular issue in mobile robotic platforms. Under the concept of team formation, these mobile robots not only can achieve more complex tasks with higher efficiency but also can expand their application fields, including environmental surveillance, reconnaissance, planetary exploration, rescue mission, payload transportation, etc [18]- [21]. However, there is still very little research to mention the collaboration among different teams or different types of mobile robotic platforms.

Nowadays, the collaborative architecture for multi-agent systems can be divided into two categories: the centralized approach and decentralized approach. In the centralized approach, there exists a powerful core unit (e.g., a robot or a computer) to determine and control the entire action of the team, which possesses both excellent global superiority and quick decision-making speed. However, once the core unit is crashed during the tracking or navigation process, the team formation cannot be maintained. In addition, if employing the centralized controller on large-scale systems, the extremely high computational complexity may cause the collaborative team formation control problem to be unsolvable, which makes the collaborative team formation system be stopped or crashed. In order to deal with these problems, the decentralized approach has been proposed to design local controller for each team formation subsystem [22], [23], [24]. In the decentralized method, each agent is only allocated specific tasks and takes actions based on their local information, which can reduce the computation cost, enhance the flexibility, and strengthen the robustness to single-agent failures.

Based on the aforementioned collaborative architecture, the team formation structure can further be classified as the following categories: leader-follower structure, behaviour-based structure, virtual structure, graph-based structure, etc [25]- [28]. At present, the leader-follower structure is still the well-recognized and popular strategy for the collaborative team formation tracking problem since its simplicity and practicality. The basic idea of leader-follower team formation structure is that some of the mobile robots are selected as leaders to track the reference trajectories, while others act as the followers to track the motion of leaders with some corresponding formation distances to achieve team formation. Therefore, under the co-design of leader-follower team formation scheme and decentralized tracking control method, the original collaborative team formation tracking control design problem can be simplified to a set of individual trajectory tracking control design problems for each leader-follower team formation subsystem. Moreover, owing to the characteristic of the decentralized team formation tracking control approach, apart from executing the commands from the leader, the followers can make decisions by themselves to bring off the obstacle avoidance.

In general, during the team formation tracking process, the dynamic system of the agent in the team formation will inevitably suffer from the unknown external disturbances such as the load variations, unmodelled forces in the robotic dynamic system [29], or coupling effects such as the communication co-channel interference between the agents [23]. In this situation, the robust H_∞ control strategy has been proposed to attenuate the effect of these unknown noises and external disturbances on the dynamic system, and applied to signal processing, system biology, financial engineering, robotics, etc [30]- [33]. Furthermore, with the help of robust H_∞ control strategy, the designer does not need to know the information of external disturbance to efficiently attenuate the effect of external disturbance with a simple design procedure.

In this study, the collaborative team formation system of hybrid teams of biped robots and tractor-trailers, which are composed of a number of hybrid team formation subsystems, is studied. Each hybrid team formation subsystem consists of a tractor-trailer as the leader and a group of biped robots as followers. In addition, the tractor-trailers (i.e., leaders) also collaborate in a leader-follower team formation structure with a desired team formation for some common task. For example, in each hybrid team formation subsystem, the leader (i.e., tractor-trailer) plays the role of determining the attack route, environmental surveillance, reconnaissance, resource supply, etc, and the followers (i.e., biped robots) receive the information from the leader and execute the attack task.

Futher, each hybrid team formation subsystem collaborates through leaders' team formation to finish common mission of task force in the future battle field. In general, it is very difficult to achieve the desired collaborative team formation tracking control design for large-scale biped robots and tractor-trailers which are divided into different hybrid team formation subsystems under external disturbances and communication couplings. In this study, the desired collaborative team formation of hybrid teams of tractor-trailers and biped robots can be prescribed through adequate reference models with the desired team formation shape embedded in the reference input; at first, a set of reference models are specified for leaders (i.e., tractor-trailer) with a desired formation shape embedded in the reference inputs to form a desired formation of leaders at the steady state, then a set of reference models with a desired formation in their reference inputs are specified for a set of followers (i.e., biped robot) to follow each leader (i.e., tractor-trailer) to form a desired formation at the steady state. Accordingly, to avoid the complex model reference tracking design, the decentralized collaborative team formation control design problem is reduced to an independent model reference tracking problem for each tractor-trailer and biped robot in each hybrid team. Afterwards, to deal with the effect of unknown external disturbances and communication couplings of collaborative team formation, the robust H_∞ decentralized collaborative team formation tracking control strategy is proposed to achieve the desired team formation of each tractor-trailer (i.e, leader) and biped robots (i.e., followers) in each hybrid team. Nevertheless, since the aforementioned robust H_∞ decentralized tracking control strategy for collaborative team formation involves in tractor-trailer dynamics, biped robot dynamics, communication couplings and a great variety of external disturbances, it is too difficult to directly design the robust H_∞ decentralized collaborative team formation tracking control strategy. Consequently, a general augmented nonlinear reference tracking error dynamic system with decentralized leader-follower structure is proposed for each leader and each follower in each hybrid team such that the robust H_∞ decentralized collaborative team formation tracking problem can be equivalently transformed to a set of Hamilton-Jacobi-inequality (HJI) -constrained problems. Nonetheless, to the best of the authors' knowledge, there still does not exist an efficient method to solve the HJI-constrained problems directly, neither analytically nor numerically. Therefore, a numerical linear parameter-varying (LPV) modeling method [34]- [37] is introduced to efficiently approximate the general augmented collaborative team formation error dynamic system such that the original HJI-constrained problems can be transformed into a set of equivalent linear matrix-inequality (LMI)-constrained problems which can be easily solved via MATLAB LMI TOOLBOX. Eventually, the simulation results of a collaborative team formation control design of three hybrid teams with one tractor-trailer as the leader and six biped robots as followers in each hybrid team are provided with comparison to demonstrate the effectiveness of the proposed robust H_∞ decentralized collaborative team formation tracking control strategy.

The contributions of this study are described as follows:

1) Novel reference models with adequate time-varying team formation offsets are proposed to produce the desired collaborative time-varying team formation of hybrid teams of tractor-trailers and biped robots. Therefore, the collaborative time-varying team formation tracking control design problem can be simplified as a robust decentralized model reference tracking control design problem under the effects of external disturbance and communication coupling for each agent.
2) A general augmented nonlinear reference tracking error dynamic system with decentralized leader-follower structure for hybrid teams of tractor-trailers and biped robots is proposed so that the collaborative time-varying team formation tracking control design problem can be transformed to a robust stabilization problem of the augmented tracking error dynamic system to simplify the design procedure of collaborative team formation tracking control strategy for collaborative teams, and each hybrid team formation subsystem consists of a tractor-trailer as the leader and a group of biped robots as followers.
3) A robust H_∞ decentralized collaborative team formation tracking control strategy is proposed to efficiently attenuate the effect of unavailable external disturbance and coupling on the tracking control performance of the collaborative team formation system. Moreover, by the proposed robust H_∞ decentralized collaborative team formation tracking control strategy, the number of the hybrid teams and the scale of followers in a hybrid team can be increased to a very large scale.
4) Based on the general augmented nonlinear reference tracking error dynamic system with leader-follower structure, the robust H_∞ decentralized collaborative team formation tracking control design problem can be equivalently transformed into a set of independent HJIs. Subsequently, by utilizing the numerical linear parameter-varying (LPV) modeling method to approximate the nonlinear team formation tracking error dynamic system, the complex HJI of each agent can be equivalently transformed to a set of LMIs, which can be easily solved for collaborative team formation tracking control of hybrid teams of biped robots and wheeled vehicles with trailers via MATLAB LMI TOOLBOX.

The study is organized as follows. In Section II, tractor-trailer dynamic system, biped-robot hybrid task/joint dynamic system in the collaborative team formation system and the corresponding preliminaries are introduced. In Section III, a collaborative team formation system with leader-follower structure with consideration of unknown external disturbance and wireless communication coupling is constructed. In Section IV, a general augmented collaborative team formation tracking error dynamic system with leader-follower structure is constructed, and a robust H_∞ decentralized collaborative team formation tracking control strategy is proposed such that the robust H_∞ decentralized collaborative team formation tracking control design problem is equivalently transformed into a set of HJI-constrained problems. In Section V, based on the numerical LPV modeling method, the complicated HJI-constrained problem of each agent is transformed into a set of LMI-constrained problems. In Section VI, a simulation example of a collaborative team formation tracking task with comparison is provided to verify the effectiveness of the proposed robust H_∞ decentralized collaborative team formation tracking control strategy. In this simulation, three hybrid teams are asked to track a desired collaborative team formation trajectory to achieve a desired team formation shape, and each hybrid team consists of one tractor-trailer (i.e., leader) and six biped robots (i.e., followers). Eventually, the conclusion is made in Section VII.

Notation 1: For a tractor-trailer in Fig. 1, P_0 is the midpoint of the two parallel plating wheels of the tractor and P_1 is the midpoint of the two parallel plating wheels of the trailer. P_{0c} is the center of mass (COM) of tractor. P_{1c} is the COM of trailer. l_0 is the distance between P_0 and P_{0c}. l_1 is the distance between P_1 and P_{1c}. d is the distance between P_0 and P_1. b is half of the distance between parallel wheels. (x_{t0}, y_{t0}) is the position of tractor. (x_{t1}, y_{t1}) is the position of trailer. $I_{\phi 0}$ is the mass moment of the tractor. $I_{\phi 1}$ is the mass moment of the trailer. m_{t0}, m_{t1}, m_{wL} and m_{wR} are the mass of tractor, trailer, left wheel, and right wheel, respectively. r is the radius of the wheel.

Notation 2: A^T (A^{-1}): the transpose (inverse) of matrix A. $A > 0$ $(A > 0)$: a positive (negative) definite matrix. $diag(A_1, A_2, \cdots, A_n)$: a block diagonal matrix with main diagonal blocks $A_1, A_2, \cdots, A_n$. C^n: the space contains the functions which have nth continuous derivatives. If the dimensions of the matrices are not given, they are assumed to have appropriate dimensions for algebra operation.

II. PRELIMINARIES OF TRACTOR-TRAILER AND BIPED ROBOT

In this study, tractor-trailer plays the role of resource supply, reconnaissance, environmental surveillance, and route planning and therefore is considered as the leader in a hybrid team. Biped robots receive information to execute some task and therefore play the role of follower in a hybrid team. In addition, the collaborative team formation system consists of several cooperative hybrid teams and each hybrid team is composed of a tractor-trailer as the leader and a group of biped robots as followers for some common task. In this section, the dynamic systems of the tractor-trailer and biped robot in the collaborative team formation are established. For the convenience of dynamic analysis, some physical constraints and assumptions are given. Therefore, more general state-space dynamic models of the tractor-trailer and biped robot are needed for the collaborative team formation tracking control design.

A. TRACTOR-TRAILER

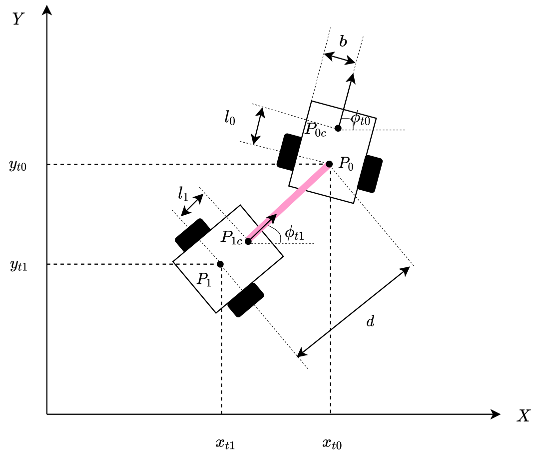

FIGURE 1: The coordinate configuration of wheeled vehicles with trailer (i.e., leader).

As shown in Fig. 1, a tractor-trailer system consists of one active driven mobile vehicle (i.e., tractor) and one passive following mobile vehicle (i.e., trailer). These two entries of the tractor-trailer system are connected by a planar rigid linkage mechanism where one end is flexible on the tractor and the other one is fixed on the trailer. In the article, the tractor has two active wheels which are driven by DC motors to control the linear velocity and angular velocity of the tractor. In contrast, the wheels of the trailer are passive. In this situation, the linear velocity and angular velocity of the trailer are driven by the rigid linkage which is connected between the tractor and the trailer.

To simplify the dynamic model of the tractor-trailer system, some physical constraints and corresponding assumptions are proposed in the following [14], [38]:

Assumption II.A.1: The running wheels of the tractor-trailer satisfy with the pure rolling condition in a forward direction and non-slipping condition in a lateral direction.

Assumption II.A.2: The inertia matrix $M_t(\cdot)$ and the Jacobian matrix $J_t(\cdot)$ of the tractor-trailer are always well-conditioned matrices with sinusoidal elements to avoid the singularity.

Assumption II.A.3: For the convenience of design, let P_0 and P_1 be the position of the tractor and trailer, respectively.

To begin with, a state-space representation for the tractor-trailer system can be defined as follows:

$$X_t(t) = [x_{t,1}(t)\ y_{t,1}(t)\ \phi_{t,1}(t)\ \phi_{t,0}(t)]^T \tag{1}$$

where $x_{t,1}(t)$ is the position of the trailer on the x-axis of the inertial frame, $y_{t,1}(t)$ is the position of the trailer on the y-axis of the inertial frame, $\phi_{t,1}(t)$ and $\phi_{t,0}(t)$ are the orientation of trailer and tractor along the z-axis with respect to the inertial frame, respectively.

Based on (1), an Euler-Lagrange-based dynamic model of the tractor-trailer system can be formulated in the following equation [14]:

$$\begin{aligned} &M_t(X_t(t))\ddot{X}_t(t) + H_t(X_t(t), \dot{X}_t(t)) \\ &= B_t(X_t(t))(\tau_t(t) + \tau_{t,ext}(t)) + A_t^T(X_t(t))\lambda \end{aligned} \tag{2}$$

where $\tau_t(t) \in \mathbb{R}^2$ is the actuator-torque vector of the tractor wheels, $\tau_{t,ext}(t) \in \mathbb{R}^2$ is the external actuator-torque vector due to unknown load variations, unmodeled friction dynamics, ground reaction forces, etc. λ is the Lagrange multiplier. $M_t(\cdot) \in \mathbb{R}^{4\times4}$ is the inertia matrix of the tractor-trailer system; $H_t(\cdot,\cdot) \in \mathbb{R}^4$ is the vector of Coriolis, centripetal and gravity forces of the tractor-trailer system; $B_t(\cdot) \in \mathbb{R}^{4\times2}$ is the input transformation matrix of the tractor-trailer system.

However, in (2), due to the existence of constraint force $A_t^T(X_t(t))\lambda$, it is very difficult to analyze the dynamic model of the tractor-trailer system. Therefore, in order to eliminate the constraint force $A_t^T(X_t(t))\lambda$, the nonholonomic constraint and Jacobian transformation are discussed and employed in the following. Firstly, based on *Assumption II.A.1* and *Assumption II.A.3*, the nonholonomic constraints from which the tractor-trailer system suffers can be written in a matrix equation as follows:

$$\begin{aligned} &A_t(X_t(t))\dot{X}_t(t) \\ &= \begin{bmatrix} \sin\phi_{t,0}(t) & \sin\phi_{t,1}(t) \\ -\cos\phi_{t,0}(t) & -\cos\phi_{t,1}(t) \\ -d\cos(\phi_{t,0}(t)-\phi_{t,1}(t)) & 0 \\ 0 & 0 \end{bmatrix}^T \\ &\times \begin{bmatrix} \dot{x}_{t,1}(t) \\ \dot{y}_{t,1}(t) \\ \dot{\phi}_{t,1}(t) \\ \dot{\phi}_{t,0}(t) \end{bmatrix} = 0 \end{aligned} \tag{3}$$

where $A_t(X_t(t))$ is the constraint matrix of the tractor-trailer system.

Subsequently, since the tractor-trailer system is driven by the linear velocity and angular velocity of tractor, the input velocity vector of the tractor-trailer system can be defined as follows:

$$\mathcal{V}_t(t) = [v_{t,0}(t)\ \dot{\phi}_{t,0}(t)]^T \in \mathbb{R}^2 \tag{4}$$

where $v_{t,0}(t)$ and $\dot{\phi}_{t,0}(t)$ are the linear velocity and the angular velocity of the tractor, respectively. Furthermore, both $v_{t,0}(t)$ and $\dot{\phi}_{t,0}(t)$ are driven by the tractor wheels, and the relationship between previous input velocity vector and the angular velocity of tractor wheels can be governed by the following equations:

$$\begin{aligned} v_{t,0}(t) &= \frac{r}{2}(\dot{\alpha}_l(t) + \dot{\alpha}_r(t)) \\ \dot{\phi}_{t,0}(t) &= \frac{r}{2b}(\dot{\alpha}_l(t) - \dot{\alpha}_r(t)) \end{aligned} \tag{5}$$

where $\dot{\alpha}_l(t)$ is the angular velocity of the tractor's left wheel, $\dot{\alpha}_r(t)$ is the angular velocity of the tractor's right wheel.

Consequently, from (1), (3) and (4), the Jacobian transformation between the state-space vector in (1) and input velocity vector in (4) can be defined as follows:

$$\dot{X}_t(t) = J_t(X_t(t))\mathcal{V}_t(t) \tag{6}$$

where $J_t(X_t(t)) \in \mathbb{R}^{4\times2}$ is the Jacobian matrix of the tractor-trailer system as follows:

$$\begin{aligned} &J_t(X_t(t)) \\ &= \begin{bmatrix} \cos\phi_{t,1}(t)\cos(\phi_{t,0}(t)-\phi_{t,1}(t)) & 0 \\ \sin\phi_{t,1}(t)\cos(\phi_{t,0}(t)-\phi_{t,1}(t)) & 0 \\ \frac{1}{d}\sin(\phi_{t,0}(t)-\phi_{t,1}(t)) & 0 \\ 0 & 1 \end{bmatrix} \end{aligned} \tag{7}$$

As a result, from (3) and (6), it can be straightforward held that:

$$J_t^T(X_t(t))A_t^T(X_t(t)) = 0 \tag{8}$$

Moreover, by differentiating (6) w.r.t time, it is clear that:

$$\ddot{X}_t(t) = \dot{J}_t(X_t(t))\mathcal{V}_t(t) + J_t(X_t(t))\dot{\mathcal{V}}_t(t) \tag{9}$$

Eventually, multiplying (2) with transpose Jacobian matrix $J_t^T(X_t(t))$, from (8), the constraint forces $A^T(X(t))\lambda$ are eliminated and the dynamic model of tractor-trailer system (2) can be reformulated in the following equation:

$$\begin{aligned} &J_t^T(X_t(t))M_t(X_t(t))\ddot{X}_t(t) + J_t^T(X_t(t))H_t(X(t), \dot{X}_t(t)) \\ &= J_t^T(X_t(t))B_t(X_t(t))(\tau_t(t) + \tau_{t,ext}(t)) \end{aligned} \tag{10}$$

Afterwards, by substituting (6) and (9) into (10), the above dynamic model can be concluded as follows:

$$\begin{aligned} &\bar{M}_t(X_t(t))\dot{\mathcal{V}}_t(t) + \bar{H}_t(X(t), \mathcal{V}_t(t)) \\ &= \bar{B}_t(X_t(t))(\tau_t(t) + \tau_{t,ext}(t)) \end{aligned} \tag{11}$$

where

$$\begin{aligned} \bar{M}_t(X_t(t)) &= J_t^T(X_t(t))M_t(X_t(t))J_t(X_t(t)) \\ \bar{H}_t(X_t(t), \mathcal{V}_t(t)) &= J_t^T(X_t(t))H_t(X(t), J_t(X_t(t))\mathcal{V}_t(t)) \\ &\quad + J_t^T(X_t(t))M_t(X_t(t))\dot{J}_t(X_t(t))\mathcal{V}_t(t) \\ \bar{B}_t(X_t(t)) &= J_t^T(X_t(t))B_t(X_t(t)) \end{aligned}$$

Furthermore, considering the dynamic model for the tractor-trailer system (11) in the nominal case by replacing the true dynamic functional matrices with their nominal values as follows:

$$\begin{aligned} &\bar{M}_t(\cdot) = \bar{M}_{t,o}(\cdot), \bar{H}_t(\cdot,\cdot) = \bar{H}_{t,o}(\cdot,\cdot) \\ &\bar{B}_t(\cdot) = \bar{B}_{t,o}(\cdot), J_t(\cdot) = J_{t,o}(\cdot), \tau_{t,ext}(t) = 0 \end{aligned} \tag{12}$$

where $\bar{M}_{t,o}(X_t(t))$ is assumed to be a symmetric positive definite functional matrix.

Therefore, based on (11) and (12), the inverse dynamics for the tractor-trailer system can be obtained on-line by computed torque method [39] and constructed as follows:

$$\begin{aligned} \tau_{inv,t}(t) &= ID_t(\dot{\mathcal{V}}_{td}(t), \mathcal{V}_t(t), X_t(t)) \\ &\triangleq \bar{B}_{t,o}^{-1}(\bar{M}_{t,o}(X_t(t))\dot{\mathcal{V}}_{td}(t) + \bar{H}_{t,o}(X_t(t), \mathcal{V}_t(t))) \end{aligned} \tag{13}$$

where the inverse dynamics $ID_t(\cdot,\cdot,\cdot)$ is used to find out the nominal actuator-torque $\tau_{inv,t}(t)$ to produce the desired acceleration $\dot{\mathcal{V}}_{td}(t)$ based on current states $\mathcal{V}_t(t)$ and $X_t(t)$. In other words, the nominal torque $\tau_{inv,t}(t)$ acts as feed-forward control torque in the controller design of the collaborative team formation tracking control design problem whose details will be introduced in the following section.

B. BIPED ROBOT

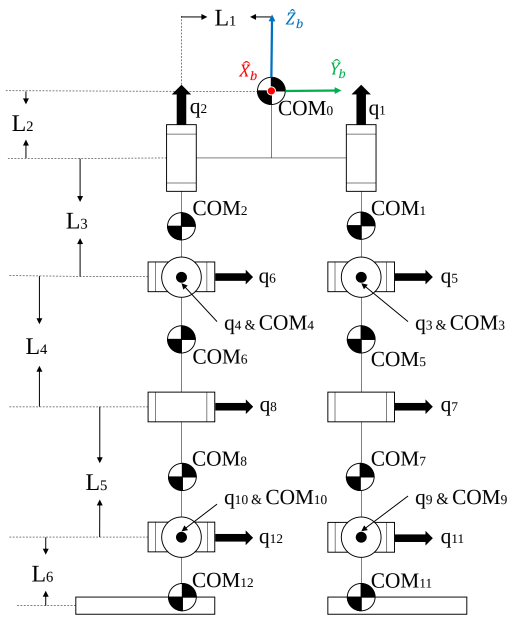

FIGURE 2: Kinematic diagram of biped robot in the neutral posture

As shown in Fig. 2, in the study, a biped robot system consists of one rigid body and two legs. Each leg is composed of six revolute joints which are connected by rigid linkage. Additionally, each revolute joint is driven by one DC motor. Further, by the symmetric properties of the biped robot mechanical configuration, the biped robot system can be regarded as a rigid multi-body dynamic system with two open series chains [40].

For the convenience of dynamic analysis, the following assumptions are given [40]:

Assumption II.B.1: The reference joint-space trajectories of biped robots are designed to ensure the non-singularity of the biped robot systems for all the desired walking leg motions to be performed, such that the inertia matrix $M_R(\cdot)$ and the body Jacobian $J_b(\cdot)$ of the biped robot system can be always considered as well-conditioned square matrices with sinusoidal elements.

Assumption II.B.2: For convenience, let the position of the mass center of rigid body COM_0 be the position of the biped robot. Moreover, COM_0 is also regarded as the body-frame center of the biped robot system.

To begin with, since the biped robot system is regarded as a rigid multi-body dynamic system with two open series chains, a hybrid task/joint dynamic model of the biped robot system is defined as follows [29]:

$$M_R(q(t))\ddot{q}(t) + H_R(q(t),\dot{q}(t)) = \tau_R(t) + \tau_{R,ext}(t) \quad (14)$$

$$\mathcal{V}_{leg}(t) = J_b(S_1 q(t))S_1\dot{q}(t) \quad (15)$$

$$\dot{X}_R(t) = G(S_2 X_R(t), q(t))\mathcal{V}_{leg}(t) \quad (16)$$

where $q(t), \dot{q}(t), \ddot{q}(t) \in \mathbb{R}^{12}$ are the angular position, angular velocity, and angular acceleration vector of revolute joints, respectively; $\tau_R(t) \in \mathbb{R}^{12}$ is the actuator-torque vector on each revolute joint; $\tau_{R,ext}(t) \in \mathbb{R}^{12}$ is the external joint torque vector due to unknown load variation, unmodeled forces, ground reaction forces, etc. $M_R(\cdot) \in \mathbb{R}^{12\times 12}$ is the inertia matrix of the biped robot system; $H_R(\cdot,\cdot) \in \mathbb{R}^{12}$ is the vector of Coriolis, centripetal and gravity forces of the biped robot system. $\mathcal{V}_{leg}(t) \in \mathbb{R}^{8}$ is the leg spatial velocity vector and is composed of three translational velocities along x, y, z-axis and one angular velocity along the z-axis of both ankle joints. Based on *Assumption II.B.1,* $J_b(\cdot)$ is the corresponding body Jacobian matrix between leg spatial velocity and angular joint velocity. At the same time, based on *Assumption II.B.2,* $X_R(t) = [x_R(t), y_R(t), \phi_R(t)]^T \in \mathbb{R}^3$ is the planar representation of position and orientation of the biped robot, i.e., $x_R(t)$ is the position of the biped robot on the x-axis of the inertial frame, $y_R(t)$ is the position of the biped robot on the y-axis of the inertial frame, and $\phi_R(t)$ is the orientation along the z-axis with respect to the inertial frame; $G(\cdot,\cdot) \in \mathbb{R}^{3\times 8}$ is the linear transformation matrix mapping from leg spatial velocity vector $\mathcal{V}_{leg}(t)$ to the linear and angular velocity of planar representation $\dot{X}_R(t)$; $S_1 = [I_8\ 0_{8\times 4}]$; $S_2 = [0_{1\times 2}\ I_1]$.

Subsequently, from (15), the Jacobian transformation between leg spatial velocity and angular joint velocity can be rewritten as follows:

$$\dot{q}(t) = J_E(q(t))\mathcal{V}_h(t) \quad (17)$$

where $\mathcal{V}_h(t) = [\mathcal{V}_{leg}^T(t)\ ([0_{4\times 8}\ I_4]\dot{q}(t))^T]^T \in \mathbb{R}^{12}$ is the hybrid task/joint velocity vector of the biped robot system; $J_E(q(t)) = diag(J_b^{-1}(S_1 q(t)), I_4) \in \mathbb{R}^{12\times 12}$ is the extended inverse Jacobian matrix of the biped robot system.

Moreover, by differentiating (17) w.r.t. time, it is clear that:

$$\ddot{q}(t) = \dot{J}_E(q(t))\mathcal{V}_h(t) + J_E(q(t))\dot{\mathcal{V}}_h(t) \quad (18)$$

Afterwards, by substituting (17) and (18) into (14), the hybrid task/joint space dynamic model of the biped robot system can be reformulated in the following equation:

$$\begin{aligned} &M_R(q(t))(\dot{J}_E(q(t))\mathcal{V}_h(t) + J_E(q(t))\dot{\mathcal{V}}_h(t)) \\ &+H_R(q(t), J_E(q(t))\mathcal{V}_h(t)) = \tau_R(t) + \tau_{R,ext}(t) \end{aligned} \quad (19)$$

$$\dot{X}_R(t) = G(S_2 X_R(t), q(t))S_1\mathcal{V}_h(t) \quad (20)$$

Furthermore, the hybrid task/joint space dynamics for biped robot system (19) in the nominal case is considered by replacing the true dynamic functions and matrices with their nominal values as follows:

$$M_R(\cdot) = M_{R,o}(\cdot), H_R(\cdot,\cdot) = H_{R,o}(\cdot,\cdot) \quad (21)$$
$$J_R(\cdot) = J_{R,o}(\cdot), \tau_{R,ext}(t) = 0$$

where $M_{R,o}(\cdot)$ is assumed to be a symmetric positive definite functional matrix.

From (19) and (21), the inverse dynamics for the biped robot system can be constructed as follows:

$$\begin{aligned}\tau_{inv,R}(t) &= ID_R(\dot{\mathcal{V}}_{hd}(t), \mathcal{V}_h(t), q(t)) \quad (22)\\ &\triangleq M_{R,o}(q(t))(\dot{J}_{E,o}(q(t))\mathcal{V}_h(t) + J_{E,o}(q(t))\dot{\mathcal{V}}_{hd}(t))\\ &+ H_{R,o}(q(t), J_{E,o}(q(t))\mathcal{V}_h(t))\end{aligned}$$

where the inverse dynamics $ID_R(\cdot,\cdot,\cdot)$ is used to find out the nominal actuator-torque $\tau_{inv,R}(t)$ to produce the desired hybrid acceleration $\dot{\mathcal{V}}_{hd}(t)$ based on current states $\mathcal{V}_h(t)$ and $q(t)$.

III. COLLABORATIVE TEAM FORMATION WITH DECENTRALIZED LEADER-FOLLOWER STRUCTURE

Most of the time, a single tractor-trailer or a single biped robot has many limitations on its applications. Therefore, many collaborative structures are proposed and realized for more practical applications in recent years [41]- [44]. However, there are still very little researches to discuss hybrid team collaboration (i.e., the collaboration among different hybrid teams where each hybrid team is composed of a tractor-trailer as the leader and a group of biped robots as followers). By the collaboration of each hybrid team, more complex and challenging tasks can be accomplished, such as searching and rescue missions, payload transportation, and planetary exploration, etc. Nevertheless, due to the high dimensional state-space of large-scale dynamic systems and complex interactions among hybrid team subsystems, the traditional centralized collaborative architecture has a very high computational cost and is very difficult to be analyzed and designed. As a result, in the section, a decentralized leader-follower team formation structure is proposed to be implemented on each hybrid team to avoid the above-mentioned problems and simplify the control design procedure in the following section.

Under the concept of decentralized leader-follower team formation structure, the leader system of tractor-trailers determines the desired trajectory of the team, and the follower systems of biped robots are asked to track the leaders' trajectories with specific distances through decentralized tracking control processing. In addition, with the help of wireless communication techniques, in each hybrid team, as shown in Fig.3, the leader (i.e., tractor-trailer) not only can send messages or commands to all followers (i.e.,biped robots) in the same hybrid team but also communicates with other leaders in different hybrid teams. Due to the characteristic of leader-follower team formation structure, even though the followers in each hybrid team can not send messages to the leader, they still can communicate with other followers in the same hybrid team. Consequently, the following assumptions are given to simplify the decentralized leader-follower structure [29]:

Assumption III.A.1: From the viewpoint of graph theory, there exists a communication link from the leader to the followers in the same hybrid team. In addition, there also exist communication links between leaders in different hybrid teams and between the followers in the same hybrid team.

Assumption III.A.2: Packet dropout and network-induced time delay are not considered in the wireless communication link, i.e., every follower can directly receive the real-time information from the leader in the same hybrid team.

Assumption III.A.3: The effects of wireless interaction couplings only exist among the agents who can communicate with each other (i.e., the leaders in the different hybrid teams, and the followers in the same hybrid team).

At first, in each hybrid team, a tractor-trailer is assigned as the leader agent and a group of biped robots are assigned as follower agents in each hybrid team. Therefore, a general leader-follower state-space representation for the leader in the ith hybrid team $X_{0,i}(t)$ and the jth follower in the ith hybrid team $X_{j,i}(t)$ of the collaborative team formation system can be defined as follows:

$$X_{0,i}(t) = [X_{t,i}^T(t)\ \mathcal{V}_{t,i}^T(t)]^T \in \mathbb{R}^{n_L}, \text{for } i \in \mathbb{N}_T \quad (23)$$

$$X_{j,i}(t) = [q_{j,i}^T(t)\ X_{R,j,i}^T(t)\ \mathcal{V}_{h,j,i}^T(t)]^T \in \mathbb{R}^{n_F}, \text{for } i \in \mathbb{N}_T,\ j \in \mathbb{N}_{F_i} \quad (24)$$

where $X_{t,i}(t)$ and $\mathcal{V}_{t,i}(t)$ are position and velocity state vectors of the leader in the ith hybrid team, respectively; $n_L = 6$ is the dimensional index of leader; $\mathbb{N}_T \triangleq \{1, 2, \cdots, N_T\}$ is the set of identity number of hybrid team; N_T is the total amount of hybrid teams in the collaborative team formation system. $q_{j,i}^T(t), X_{R,j,i}^T(t), \mathcal{V}_{h,j,i}^T(t)$ are the state vectors of angular positions of revolute joints, planar representation of position and orientation, and hybrid velocity of the jth follower in the ith hybrid team, respectively; $n_F = 27$ is the dimensional index of biped robot; $\mathbb{N}_{F_i} \triangleq \{1, 2, \cdots, N_i\}$ is the set of identity number of biped robot; N_i is the total amount of followers in the ith hybrid team (i.e., the number of followers in each hybrid team can be different).

Based on *Assumption III.A.1* to *Assumption III.A.3* and the state vectors in (23) and (24), the dynamic model of the leader and the jth follower in the ith hybrid team of the collaborative team formation system can be formulated as follows:

$$\begin{aligned}\dot{X}_{0,i}(t) &= f_{0,i}(X_{0,i}(t)) + g_{0,i}(X_{0,i}(t))U_{0,i}(t)\\ &+ \upsilon_{0,i}(t) + \sum_{j=1,j\neq i}^{N_T} f_{0,j,i}(X_{0,i}(t))X_{0,j}(t) \quad (25)\\ &, \text{for } i \in \mathbb{N}_T\end{aligned}$$

$$\begin{aligned}\dot{X}_{j,i}(t) &= f_{j,i}(X_{j,i}(t)) + g_{j,i}(X_{j,i}(t))U_{j,i}(t)\\ &+ \upsilon_{j,i}(t) + \sum_{k=1,k\neq j}^{N_i} f_{j,k,i}(X_{j,i}(t))X_{k,i}(t) \quad (26)\\ &, \text{for } i \in \mathbb{N}_T,\ j \in \mathbb{N}_{F_i}\end{aligned}$$

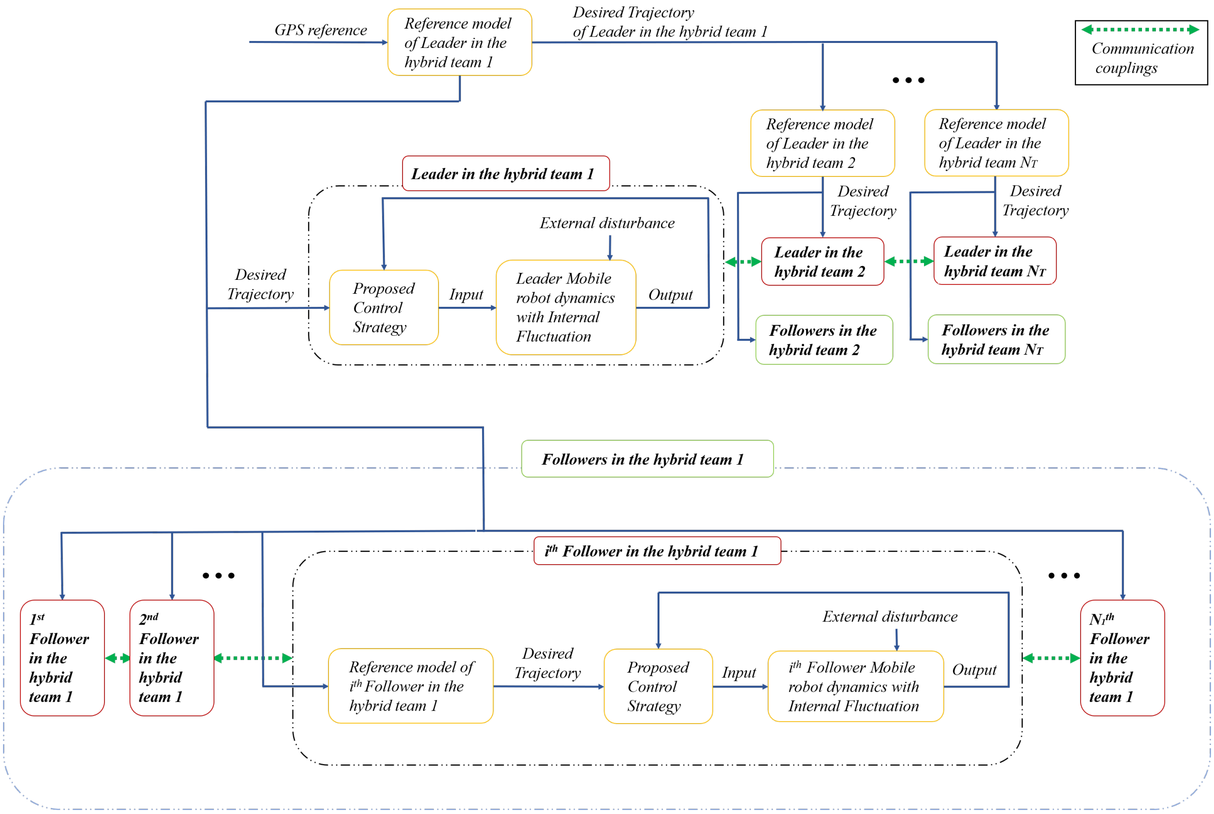

FIGURE 3: The structure of the collaborative team formation system with decentralized leader-follower structure for the hybrid teams of tractor-trailer and biped robots.

with

$$f_{0,i}(X_{0,i}(t)) = \begin{bmatrix} J_{t,i}(X_{t,i}(t))\mathcal{V}_{t,i}(t) \\ -\bar{M}_{t,i}^{-1}(X_{t,i}(t))\bar{H}_{t,i}(X_{t,i}(t),\mathcal{V}_{t,i}(t)) \end{bmatrix}$$

$$g_{0,i}(X_{0,i}(t)) = \begin{bmatrix} 0 \\ \bar{M}_{t,i}^{-1}(X_{t,i}(t))\bar{B}_{t,i}(X_{t,i}(t)) \end{bmatrix}$$

$$\upsilon_{0,i}(t) = \begin{bmatrix} 0 \\ \bar{M}_{t,i}^{-1}(X_{t,i}(t))\bar{B}_{t,i}(X_{t,i}(t))\tau_{t,ext,i}(t) \end{bmatrix} + \omega_{0,i}(t)$$

$$f_{j,i}(X_{j,i}(t)) = \begin{bmatrix} J_{E,j,i}(q_{j,i}(t))\mathcal{V}_{h,j,i}(t) \\ G_{j,i}(S_2X_{R,j,i}(t),q_{j,i}(t)) \\ \times S_1\mathcal{V}_{h,j,i}(t) \\ J_{E,j,i}^{-1}(q_{j,i}(t))(-M_{R,j,i}^{-1}(q_{j,i}(t)) \\ \times H_{R,j,i}(q_{j,i}(t),J_{E,j,i}(q_{j,i}(t)) \\ \times \mathcal{V}_{h,j,i}(t)) - \dot{J}_{E,j,i}(q_{j,i}(t)) \\ \times \mathcal{V}_{h,j,i}(t)) \end{bmatrix}$$

$$g_{j,i}(X_{j,i}(t)) = \begin{bmatrix} 0 \\ J_{E,j,i}^{-1}(q_{j,i}(t))M_{R,j,i}^{-1}(q_{j,i}(t)) \end{bmatrix}$$

$$\upsilon_{j,i}(t) = \begin{bmatrix} 0 \\ J_{E,j,i}^{-1}(q_{j,i}(t))M_{R,j,i}^{-1}(q_{j,i}(t))\tau_{R,ext,j,i}(t) \end{bmatrix} + \omega_{j,i}(t)$$

where $U_{0,i}(t) = \tau_{t,i}(t) \in \mathbb{R}^{n_{u,0,i}}$ and $U_{j,i}(t) = \tau_{R,j,i}(t) \in \mathbb{R}^{n_{u,j,i}}$ are control input of the leader in the ith hybrid team and the jth follower in the ith hybrid team, respectively; $\upsilon_{0,i}(t)$ and $\upsilon_{j,i}(t)$ is the bounded external disturbance of the leader in the ith hybrid team and the jth follower in the ith hybrid team, respectively; $\upsilon_{0,i}(t)$ is composed of external joint torques $\bar{M}_{t,i}^{-1}(\cdot)\bar{B}_{t,i}(\cdot)\tau_{t,ext,i}(t)$ and unmodelled tractor-trailer dynamics $\omega_{0,i}(t)$. $\upsilon_{j,i}(t)$ includes external joint torques $J_{E,j,i}^{-1}(q_i(t))M_{R,j,i}^{-1}(q_i(t))\tau_{R,ext,j,i}(t)$ and unmodelled biped-robot dynamics $\omega_{j,i}(t)$; $M_{R,j,i}(\cdot)$,$H_{R,j,i}(\cdot,\cdot)$,$J_{E,j,i}(\cdot)$,$G_{j,i}(\cdot,\cdot)$ are the system functional matrices of the jth biped robot system in the the ith hybrid team. $\sum_{j=1,j\neq i}^{N_T} f_{0,j,i}(X_{0,i}(t))X_{0,j}(t)$ are the couplings from other leaders in the different hybrid team to the leader in the ith hybrid team and $\sum_{k=1,k\neq j}^{N_i} f_{j,k,i}(X_{j,i}(t))X_{k,i}(t)$ are the couplings from other followers in the ith hybrid team to the jth follower in the ith hybrid team. $n_{u,0,i} = 2$ and $n_{u,j,i} = 12$ are dimensional indices.

IV. PROBLEM FORMULATION

In this section, for the convenience of design, the augmented collaborative team formation tracking error dynamic model with decentralized leader-follower structure is utilized to deal with the collaborative team formation tracking control problem for the hybrid teams of tractor-trailers and biped robots. In this case, in order to design and generate a smooth tracking trajectory with the continuity of first and second derivatives, the reference model is proposed to prescribe the desired trajectories of collaborative team formation system.

Moreover, the schematic diagram of team formation is shown in Fig.4. In Fig.4, each hybrid team is composed of one tractor as the leader and six biped robots as followers for a task. Since the collaborative team formation control design of hybrid team is complex, more efforts are needed to specify their reference models with a desired leader-follower structure.

In the beginning, for the collaborative team formation tracking design, the desired trajectory to be tracked by the leader in the ith hybrid team is generated by the following reference model [46], [49]:

$$\dot{X}_{r,0,i}(t) = A_{r,0,i}X_{r,0,i}(t) + B_{r,0,i}r_{0,i}(t), \text{for } i \in \mathbb{N}_T \quad (27)$$

where $X_{r,0,i}(t) = [x_{d,1,i}(t), y_{d,1,i}(t), \phi_{d,1,i}(t), \phi_{d,0,i}(t), v_{d,0,i}(t), \dot{\phi}_{d,0,i}(t), \dot{\phi}_{d,1,i}(t), \dot{v}_{d,0,i}(t), \ddot{\phi}_{d,0,i}(t)]^T \in \mathbb{R}^{n_{Lr}}$ is the desired trajectory of the leader in the ith hybrid team of the collaborative team formation system and the dimensional index $n_{Lr} = 9$; $x_{d,1,i}(t)$ is the desired position of trailer in the ith hybrid team on the x-axis of the inertial frame; $y_{d,1,i}(t)$ is the desired position of trailer in the ith hybrid team on the y-axis of the inertial frame; $\phi_{d,0,i}(t)$ and $\phi_{d,1,i}(t)$ are the desired orientation of trailer and tractor in the ith hybrid team along z-axis of the inertial frame, respectively; $v_{d,0,i}(t)$ is the desired linear velocity of tractor in the ith hybrid team; $\dot{\phi}_{d,0,i}(t)$ and $\dot{\phi}_{d,1,i}(t)$ are the desired angular velocity of tractor and trailer in the ith hybrid team along z-axis of the inertial frame, respectively; $\dot{v}_{d,0,i}(t)$ and $\ddot{\phi}_{d,0,i}(t)$ are the desired linear acceleration and angular acceleration of tractor in the ith hybrid team. $r_{0,i}(t) \in \mathbb{R}^{n_{Lr}}$ is the bounded reference input of reference model, i.e., the ideal trajectory of the tractor-trailer in the ith hybrid team; $A_{r,0,i} \in \mathbb{R}^{n_{Lr} \times n_{Lr}}$ is the reference system matrix and $B_{r,0,i} \in \mathbb{R}^{n_{Lr} \times n_{Lr}}$ is the reference input matrix, both of which characterize the transient behaviour of the reference model.

Subsequently, by wireless communication technique, the followers in the collaborative team formation system can receive information from the leader in the same hybrid team. This information can be assigned as reference input of the follower's reference model. Furthermore, if there are some obstacles on the prescribed trajectories, the followers can also plan their trajecotries beforehand to avoid the collision. As a consequence, for the collaborative team formation, the reference model of the jth follower in the ith hybrid team can be given as follows:

$$\begin{aligned}\dot{X}_{r,j,i}(t) = A_{r,j,i}X_{r,j,i}(t) + B_{r,j,i}r_{j,i}(t) \\ , \text{for } i \in \mathbb{N}_T,\ j \in \mathbb{N}_{F_i}\end{aligned} \quad (28)$$

where $X_{r,j,i}(t) = [X^T_{d,j,i}(t), \dot{X}^T_{d,j,i}(t), \ddot{X}^T_{d,j,i}(t)]^T \in \mathbb{R}^{n_{Fr}}$ is the desired tracking trajectory of the jth follower in the ith hybrid team of the collaborative team formation system and the dimensional index $n_{Fr} = 9$; $X_{d,j,i}(t) = [x_{d,j,i}(t), y_{d,j,i}(t), \phi_{d,j,i}(t)]^T$; $x_{d,j,i}(t)$, $y_{d,j,i}(t)$ are the desired position of the jth biped robot in the ith hybrid team on the x-axis and y-axis of the inertial frame, respectively; $\phi_{d,j,i}(t)$ is the desired orientation of the jth biped robot in the ith hybrid team along the z-axis of the inertial frame; $\dot{X}_{d,j,i}(t)$ is the desired planar velocity vector of the jth follower in the ith hybrid team; $\ddot{X}_{d,j,i}(t)$ is the desired planar acceleration vector of the jth follower in the ith hybrid team; $r_{j,i}(t) \in \mathbb{R}^{n_{Fr}}$ is the bounded reference input of reference model which is the ideal trajectory of the jth follower in the ith hybrid team; $A_{r,j,i} \in \mathbb{R}^{n_{Fr} \times n_{Fr}}$ is the reference system matrix and $B_{r,j,i} \in \mathbb{R}^{n_{Fr} \times n_{Fr}}$ is the reference input matrix.

In general, the collaborative team formation trajectory design can be separated into two parts: the team formation of the leaders in different hybrid teams and the team formation of the followers in each hybrid team. For the team formation of the leaders in different hybrid teams, the ideal team formation trajectory of the leader in the hybrid team 1 is planned firstly and considered as the reference input $r_{0,1}(t)$ in (27). Afterwards, to achieve a prescribed team formation shape, the trajectories of other leaders should maintain specific distances relative to the trajectory of the leader in the hybrid team 1. Therefore, the ideal trajectory of the leader in the ith hybrid team of the collaborative team formation system in (27) can be designed by the following equation:

$$r_{0,i}(t) = r_{0,1}(t) + d_{0,i}(t), \text{for } i \in \mathbb{N}_T \quad (29)$$

where $d_{0,i}(t)$ is the time-varying team formation offset for the leader in the ith hybrid team, i.e., if the reference model of the leader (i.e., tractor-trailer) in the ith hybrid team in (27) is specified input $r_{0,i}(t)$ in (29), then the leader in the hybrid team i has an offset $d_{0,i}(t)$ with the leader in hybrid team 1 at the steady state.

Subsequently, for the team formation of followers in each hybrid team, each follower is asked to track the trajectory of their leader with a specific offset to achieve the prescribed team formation shape. Accordingly, the ideal trajectory of the jth follower in the ith hybrid team of the collaborative team formation system in (28) can be designed by the following equation:

$$r_{j,i}(t) = r_{0,i}(t) + d_{j,i}(t), \text{for } i \in \mathbb{N}_T,\ j \in \mathbb{N}_{F_i} \quad (30)$$

where $d_{j,i}(t)$ is the time-varying team formation offset for the jth follower in the ith hybrid team, i.e., if the reference model of the jth follower (i.e., biped robot) in the ith hybrid team in (28) is specified input $r_{j,i}(t)$ in (30), then the jth follower in the hybrid team i has an offset $d_{j,i}(t)$ with the leader in hybrid team i at the steady state.

Remark 1: In the reference model architectures of leaders in (27) and followers in (28) in the hybrid teams of the collaborative team formation, the agents in the collaborative team formation can choose their desired time-varying formation shapes in (29) or (30) as targets for tracking, to be considered as the reference inputs of their reference models. Moreover, a specific asymptotically stable matrix $A_{r,0,i}$ or $A_{r,j,i}$ is chosen to be a reference system matrix in (27) or (28). By taking the leader's reference model in (27) as an example, at the steady state, $X_{r,0,i}(t) = A^{-1}_{r,0,i}B_{r,0,i}r_{0,i}(t)$. If we choose $A_{r,0,i} = -B_{r,0,i} = -10I_9$, the desired trajectory $X_{r,0,i}(t)$ will approach to the reference input $r_{0,i}(t)$ at the steady state with a convergence rate e^{-10t}. Similarly, if we

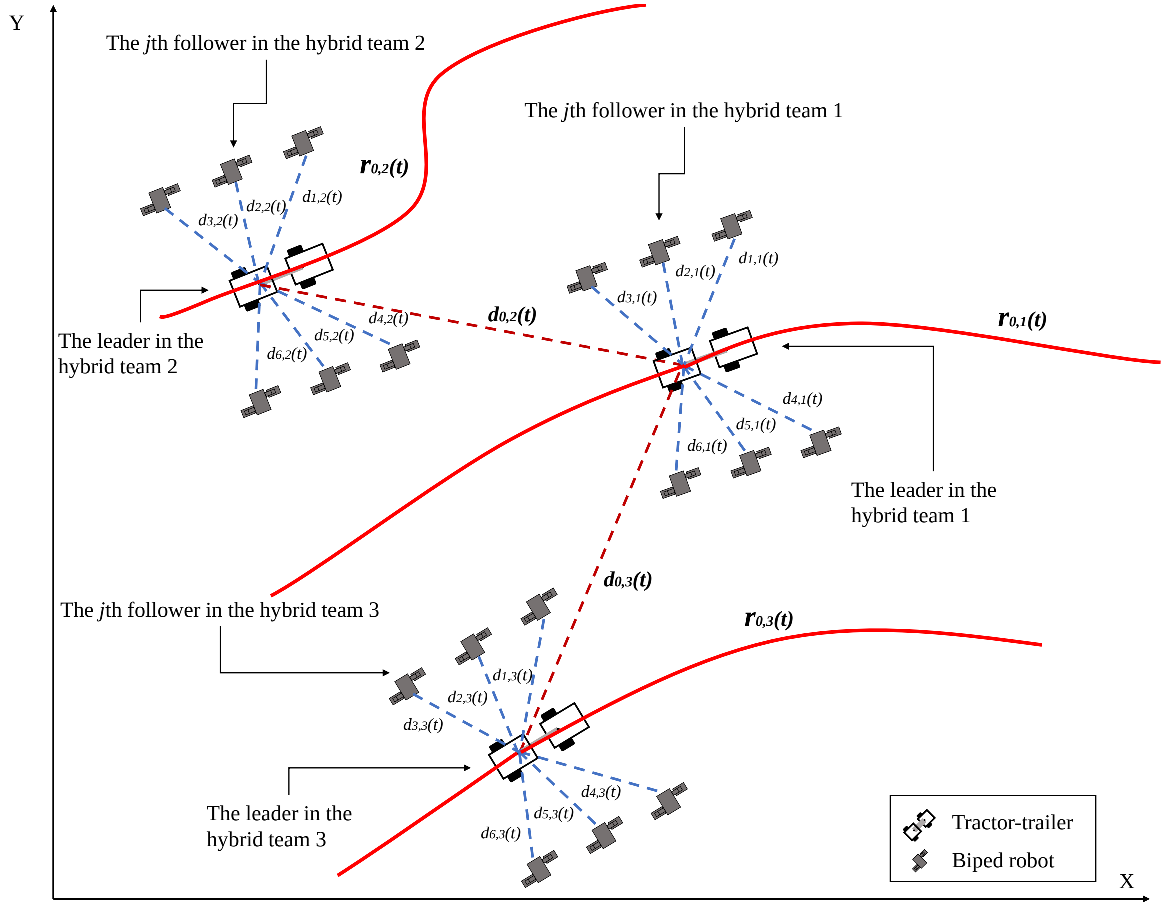

FIGURE 4: The diagram of collaborative team formation system. The white one is the tractor-trailer (i.e., leader) in the ith hybrid team. The gray ones are the biped robots (i.e., followers) in the ith hybrid team. Each hybrid team consists of one tractor-trailer as the leader and six biped robots as followers. In this figure, the leader in the hybrid team 1 is the leader system of other leaders in the hybrid team i. $r_{0,i}(t)$ denotes the desired trajectory of the tractor-trailer in the hybrid team i and $d_{0,i}(t)$ denotes the desired formation offset of the leader in the hybrid team i to its leader (i.e., the leader in the hybrid team 1) when $d_{j,i}(t)$ denotes the desired formation offset of the jth biped robot in the ith hybrid team to its leader (i.e., the leader in the hybrid team i).

choose $A_{r,j,i} = -B_{r,j,i} = -10I_9$, the desired trajectory $X_{r,j,i}(t)$ will approach to the reference input $r_{j,i}(t)$ at the steady state with a convergence rate e^{-10t}. In this situation, the team formation of N_T leaders (i.e., tractor-trailers) will result in a formation shape $(d_{0,2}(t), d_{0,3}(t), \cdots, d_{0,N_T}(t))$ w.r.t. the first tractor-trailer and the N_i followers (i.e., biped robots) of the ith hybrid team will result in a formation shape $(d_{1,i}(t), d_{2,i}(t), \cdots, d_{N_i,i}(t))$ w.r.t. their leader (i.e., the tractor-trailer in the ith team) at the steady state.

In conclusion, to cope with various requirements or tasks in hybrid teams, the corresponding ideal trajectories of the leaders and followers in the collaborative team formation can be efficiently designed by (29) and (30). Afterwards, by the reference model in (27) and (28), the smooth desired tracking trajectories for the leaders and followers in the collaborative team formation are generated immediately. Moreover, with the help of specifying adequate time-varying team formation offset $d_{0,i}(t)$ and $d_{j,i}(t)$, different from the fixed team formation shape [23], [27], some desired time-varying team formation shapes can be easily achieved by the proposed team formation reference model tracking control strategy for the leaders in the team 0 (i.e., the team formation of leaders in different hybrid teams) to track their corresponding reference models in (27) when the followers in the ith hybrid team to track their corresponding reference model in (28). Afterwards, at the steady state, the team formation of team 0 will form a desired formation shape with formation offset $d_{0,i}(t)$ and the team formation of the ith hybrid team (i.e., the team formation of the leader and the followers in the ith hybrid team) will form a desired formation shape with formation offset $d_{j,i}(t)$ simultaneously.

Remark 2: Since the desired reference models and reference inputs of each leader in (27), (29) and of each follower in (28), (30) can be specified for collaborative team formation beforehand, the complex collaborative team formation control problem of hybrid teams composed of a tractor-trailer as the leader and a group of biped robots as followers in each hybrid team can be easily designed independently by a set of decentralized reference model tracking control problems of each biped robot or tractor-trailer.

Accordingly, from the general leader state vector in (23) and the corresponding reference model in (27), a general collaborative team formation tracking error vector between the planar representation of the leader (i.e., tractor-trailer) in the ith hybrid team and its desired trajectory can be defined as follows:

$$\tilde{X}_{0,i}(t)=[\tilde{X}_{t,i}^T(t)\ \tilde{\mathcal{V}}_{t,i}^T(t)]^T, \text{for } i\in\mathbb{N}_T \tag{31}$$

with

$$\tilde{X}_{t,i}(t)=X_{t,i}(t)-S_3X_{r,0,i}(t) \tag{32}$$
$$\tilde{\mathcal{V}}_{t,i}(t)=\mathcal{V}_{t,i}(t)-S_4X_{r,0,i}(t) \tag{33}$$

where $S_3=[I_4,0_{4\times 5}]\,,S_4=[0_{2\times 4},I_2,0_{2\times 3}]$.

Thereafter, by the following transformation matrix $T(X_{r,0,i}(t))$, the original collaborative team formation position tracking error vector $\tilde{X}_{t,i}(t)$ in (32) can be substituted by a new position tracking error vector $\tilde{X}_{e,i}(t)$ as follows [38]:

$$\tilde{X}_{e,i}(t)=T(X_{r,0,i}(t))\tilde{X}_{t,i}(t), \text{for } i\in\mathbb{N}_T \tag{34}$$

with

$$T(X_{r,0,i}(t))=\begin{bmatrix}\Gamma(X_{r,0,i}(t)) & 0\\ 0 & I_2\end{bmatrix} \tag{35}$$
$$\Gamma(X_{r,0,i}(t))=\begin{bmatrix}\cos\phi_{d,1,i}(t) & \sin\phi_{d,1,i}(t)\\ -\sin\phi_{d,1,i}(t) & \cos\phi_{d,1,i}(t)\end{bmatrix} \tag{36}$$

Therefore, the original general collaborative team formation tracking error vector in (31) can be reformulated as follows:

$$\tilde{X}_{e0,i}(t)=[\tilde{X}_{e,i}^T(t)\ \tilde{\mathcal{V}}_{t,i}^T(t)]^T, \text{for } i\in\mathbb{N}_T \tag{37}$$

It is worth noticing that the original tracking error vector $\tilde{X}_{t,i}(t)$ is defined in the inertial frame, while the new tracking error vector $\tilde{X}_{e,i}(t)$ is defined in the body frame of the leader in the ith hybrid team.

For the biped robot in the collaborative team formation system, the hybrid task/joint collaborative team formation tracking error vector between the jth follower (i.e., biped robot) in the ith hybrid team and its desired trajectory can be defined as follows:

$$\tilde{X}_{j,i}(t)=[\tilde{q}_{j,i}^T(t)\ \tilde{X}_{R,j,i}^T(t)\ \mathcal{V}_{h,j,i}^T(t)]^T\\ ,\text{for } i\in\mathbb{N}_T,\ j\in\mathbb{N}_{F_i} \tag{38}$$

with

$$\tilde{q}_{j,i}(t)=S_5q_{j,i}(t) \tag{39}$$
$$\tilde{X}_{R,j,i}(t)=X_{R,j,i}(t)-S_6X_{r,j,i}(t) \tag{40}$$

where $\tilde{q}_{j,i}(t)$ is the the tracking error vector of redundant joints (i.e., the last four revolute joints) when it is to be designed to keep an upright torso while biped robot is walking as $\tilde{q}_{j,i}(t)\to 0$; $\tilde{X}_{R,j,i}(t)$ is the collaborative team formation tracking error vector between the planar representation of position vector and the desired trajectory of the jth biped robot in the ith team; $S_5=[S_1^T,[0_{4\times 2},I_4[0_2,I_2],I_4]^T]^T$; $S_6=[I_3,0_{3\times 6}]$.

In general, the external disturbance is unavoidable and significantly deteriorates the control performance of most physical systems [50], [51]. Therefore, a robust H_∞ decentralized collaborative team formation tracking control strategy is proposed to attenuate the effect of unavailable finite energy external disturbance on the team formation tracking control performance of each leader-follower hybrid team. Moreover, since the characteristic of the robust H_∞ collaborative team formation tracking control strategy is to consider the worst-case effect of all possible finite-energy external disturbances, a designer does not need the information of external disturbance for a desired external disturbance attenuation level [30]- [32]. This advantage of robust H_∞ decentralized collaborative team formation tracking control strategy will simplify the following control design procedure with a guaranteed robust tracking performance.

Therefore, as it has been noted, to attenuate the worst-case effect of external disturbance and the wireless communication coupling on the leader-follower formation of each hybrid team, the robust H_∞ decentralized collaborative team formation tracking control strategy for the leader in the ith hybrid team and the jth follower in the ith hybrid team can be defined, respectively, as follows:

$$J_{\infty,0,i}(U_{0,i}(t)) \tag{41}$$
$$=\sup_{\Theta_{0,i}}\frac{\begin{matrix}\int_0^{t_f}[\tilde{X}_{e,i}^T(t)Q_{1,0,i}\tilde{X}_{e,i}(t)\\ +\tilde{\mathcal{V}}_{t,i}^T(t)Q_{2,0,i}\tilde{\mathcal{V}}_{t,i}(t)\\ +u_{0,i}^T(t)R_{0,i}u_{0,i}(t)]dt\\ -V_{0,i}(\tilde{X}_{e0,i}(0))\end{matrix}}{\begin{matrix}\int_0^{t_f}[r_{0,i}^T(t)r_{0,i}(t)\\ +v_{0,i}^T(t)v_{0,i}(t)\\ +\sum_{j=1,j\neq i}^{N_T}X_{0,j}^T(t)X_{0,j}(t)]dt\end{matrix}}\le\rho_{0,i}^2, \text{for } i\in\mathbb{N}_T$$

$$J_{\infty,j,i}(U_{j,i}(t)) \tag{42}$$
$$=\sup_{\Theta_{j,i}}\frac{\begin{matrix}\int_0^{t_f}[\tilde{q}_{j,i}^T(t)\bar{Q}_{1,j,i}\tilde{q}_{j,i}(t)\\ +\tilde{X}_{R,j,i}^T(t)Q_{2,j,i}\tilde{X}_{R,j,i}(t)\\ +u_{j,i}^T(t)R_{j,i}u_{j,i}(t)]dt\\ -V_{j,i}(\tilde{X}_{j,i}(0))\end{matrix}}{\begin{matrix}\int_0^{t_f}[r_{j,i}^T(t)r_{j,i}(t)\\ +v_{j,i}^T(t)v_{j,i}(t)\\ \sum_{k=1,k\neq j}^{N_i}X_{k,i}^T(t)X_{k,i}(t)]dt\end{matrix}}\le\rho_{j,i}^2$$
$$,\text{for } i\in\mathbb{N}_T,\ j\in\mathbb{N}_{F_i}$$

where $\Theta_{0,i}=\left\{r_{0,i}(t),v_{0,i}(t),\sum_{j=1,j\neq i}^{N_T}X_{0,j}(t)\right\}$ and $\Theta_{j,i}=\left\{r_{j,i}(t),v_{j,i}(t),\sum_{k=1,k\neq j}^{N}X_{k,i}(t)\right\}$ are unavailable external disturbances, reference inputs and couplings on the leader in the ith hybrid team and the jth follower in the ith hybrid team, repectively; $Q_{1,0,i}>0$, $Q_{2,0,i}>0$ and $R_{0,i}>0$ with appropriate dimension are the corresponding positive weighting matrices for the leader in the ith hybrid team; $\bar{Q}_{1,j,i} = M^T Q_{1,j,i} M$ is a modified weighting matrix and $M = [0_{4\times 8}, I_4]$; $\bar{Q}_{1,j,i} > 0$, $Q_{2,j,i} > 0$ and $R_{j,i} > 0$ with appropriate dimension are the corresponding positive weighting matrices for the jth follower in the ith hybrid team. The term of $-V_{0,i}(\tilde{X}_{e0,i}(0))$ and $-V_{j,i}(\tilde{X}_{j,i}(0))$ are used to eliminate the effect of the initial condition for some Lyapunov functions with $V_{0,i}(\cdot) > 0$, $V_{j,i}(\cdot) > 0$, $V_{0,i}(\cdot) \in C^2(\mathbb{R}^{n_L})$ and $V_{j,i}(\cdot) \in C^2(\mathbb{R}^{n_F})$; t_f is the terminal time of tracking control.

For the robust H_∞ decentralized collaborative team formation tracking control strategy of leader in (41), there exists a trade-off between the team formation tracking error of leader (i.e., $\tilde{X}_{e,i}(t)$ and $\tilde{\mathcal{V}}_{t,i}(t)$) and feedback control effort of leader (i.e., $u_{0,i}(t)$). Similarly, for the robust H_∞ decentralized collaborative team formation tracking control strategy of follower in (28), there also exists a trade-off between the redundant joint tracking error of follower (i.e., $\tilde{q}_{j,i}(t)$), team formation tracking error of follower (i.e., $\tilde{X}_{R,j,i}(t)$) and feedback control effort of follower (i.e., $u_{j,i}(t)$). The details of collaborative team formation control design procedure will be illustrated in the sequal.

The physical meaning of (41) and (28) is that designing the control input of the leader in the ith hybrid team $U_{0,i}(t)$ and the control input of the jth follower in the ith hybrid team $U_{j,i}(t)$ such that the worst-case effects of unavailable external disturbances, reference inputs, and couplings in $\Theta_{0,i}$ and $\Theta_{j,i}$ on the collaborative team formation tracking error and control effort of each leader-follower formation of hybrid teams must be less than or equal to a prescribed attenuation level $\rho^2_{0,i}$ or $\rho^2_{j,i}$ to achieve a robust H_∞ decentralized collaborative team formation tracking control for each tractor-trailer (i.e., leader) and each biped robot (i.e., follower) in the collaborative team formation.

Nevertheless, the robust H_∞ decentralized collaborative team formation tracking control strategy in (41) and (42) includes tractor-trailer dynamic system, biped robot dynamic system and a variety of external disturbances. It is difficult to design a controller to achieve the decentralized team formation reference tracking performance in (41) and (42) for each leader-follower formation of hybrid teams directly. Therefore, in order to simplify the robust H_∞ decentralized leader-follower collaborative team formation tracking control design procedure, the augmented state vectors of the collaborative team formation tracking error dynamic system of the leader in the ith hybrid team and the jth follower in the ith hybrid team are denoted as follows:

$$\tilde{e}_{0,i}(t) = [X^T_{r,0,i}(t)\ \tilde{X}^T_{e0,i}(t)]^T \in \mathbb{R}^{n_{e,0,i}} \quad ,\text{for } i \in \mathbb{N}_T \tag{43}$$

$$\tilde{e}_{j,i}(t) = [X^T_{r,j,i}(t)\ \tilde{X}^T_{j,i}(t)]^T \in \mathbb{R}^{n_{e,j,i}} \quad ,\text{for } i \in \mathbb{N}_T,\ j \in \mathbb{N}_{F_i} \tag{44}$$

where $n_{e,0,i} = n_{Lr} + n_L$, $n_{e,j,i} = n_{Fr} + n_F$ are the dimensional indices.

Based on the state vector in (43) and (44), a general state-space model for augmented collaborative team formation error dynamic system of the jth leader-follower team formation subsystem in the ith hybrid team can be formulated in the following equation:

$$\begin{aligned}\dot{\tilde{e}}_{j,i}(t) &= \tilde{f}_{j,i}(\tilde{e}_{j,i}(t)) + \tilde{g}_{j,i}(\tilde{e}_{j,i}(t))U_{j,i}(t)\\ &\quad + \tilde{D}_{j,i}(\tilde{e}_{j,i}(t))\tilde{v}_{j,i}(t)\\ &\quad + \tilde{f}_{-j,i}(\tilde{e}_{j,i}(t))\tilde{X}_{-j,i}(t)\\ &\quad ,\text{for } i \in \mathbb{N}_T,\ j \in \mathbb{N}_i\end{aligned} \tag{45}$$

where $\mathbb{N}_i \triangleq \{0, 1, 2, \cdots, N_i\}$ (i.e, the general state-space model in (45) can be utilized to express the error dynamic system of the tractor-trailer and the error dynamic system of the biped robots in each hybrid team), with the following augmented vectors and error dynamic system functions:

$$\tilde{v}_{0,i}(t) = [r^T_{0,i}(t), v^T_{0,i}(t)]^T \in \mathbb{R}^{n_{v,0,i}}, \text{for } i \in \mathbb{N}_T$$
$$\tilde{v}_{j,i}(t) = [r^T_{j,i}(t), v^T_{j,i}(t)]^T \in \mathbb{R}^{n_{v,j,i}}, \text{for } i \in \mathbb{N}_T,\ j \in \mathbb{N}_{F_i}$$

$$\tilde{f}_{0,i}(\tilde{e}_{0,i}(t)) = \begin{bmatrix} A_{r,0,i}X_{r,0,i}(t) \\ T(X_{r,0,i}(t))\{\tilde{J}_{t,i}(\tilde{e}_{j,i}(t))[\tilde{\mathcal{V}}_{t,i}(t) \\ +S_4X_{r,0,i}(t)] - S_3A_{r,0,i}X_{r,0,i}(t)\} \\ +\dot{T}(X_{r,0,i}(t))T^{-1}(X_{r,0,i}(t)) \\ \times\tilde{X}_{e,i}(t) \\ -\tilde{M}^{-1}_{t,i}(\tilde{e}_i(t))\tilde{H}_{t,i}(\tilde{e}_i(t)) \\ -S_4A_{r,0,i}X_{r,0,i}(t) \end{bmatrix}$$
$$,\text{for } i \in \mathbb{N}_T$$

$$\tilde{g}_{0,i}(\tilde{e}_{0,i}(t)) = \begin{bmatrix} 0 \\ \tilde{M}^{-1}_{t,i}(\tilde{e}_{0,i}(t))\tilde{B}_{t,i}(\tilde{e}_{0,i}(t)) \end{bmatrix}$$
$$,\text{for } i \in \mathbb{N}_T$$

$$\tilde{D}_{0,i}(\tilde{e}_{0,i}(t)) = \begin{bmatrix} B_{r,0,i} & 0 \\ S_7 & S_8 \end{bmatrix}, \text{for } i \in \mathbb{N}_T$$

$$\tilde{f}_{-0,i}(\tilde{e}_{0,i}(t)) = \begin{bmatrix} 0 \\ S_8 f_{-0,i}(\tilde{e}_{0,i}(t)) \end{bmatrix}, \text{for } i \in \mathbb{N}_T$$

$$S_7 = [[-T(X_{r,0,i}(t))S_3B_{r,0,i}]^T, [-S_4B_{r,0,i}]^T,$$
$$S_8 = diag(T(X_{r,0,i}(t)), I)$$

$$\tilde{f}_{j,i}(\tilde{e}_{j,i}(t)) = \begin{bmatrix} A_{r,j,i}X_{r,j,i}(t) \\ S_5\tilde{J}_{E,j,i}(\tilde{e}_{j,i}(t))\mathcal{V}_{h,j,i}(t) \\ \tilde{G}_{j,i}(\tilde{e}_{j,i}(t))S_1V_{h,j,i}(t) \\ -S_6A_{r,j,i}X_{r,j,i}(t) \\ \tilde{J}^{-1}_{E,j,i}(\tilde{e}_{j,i}(t))[-\tilde{M}^{-1}_{R,j,i}(\tilde{e}_{j,i}(t)) \\ \times\tilde{H}_{R,j,i}(\tilde{e}_{j,i}(t)) - \dot{\tilde{J}}_{E,j,i}(\tilde{e}_{j,i}(t)) \\ \times\mathcal{V}_{h,j,i}(t)] \end{bmatrix}$$
$$,\text{for } i \in \mathbb{N}_T,\ j \in \mathbb{N}_{F_i}$$

$$\tilde{g}_{j,i}(\tilde{e}_{j,i}(t)) = \begin{bmatrix} 0 \\ \tilde{J}^{-1}_{E,j,i}(\tilde{e}_{j,i}(t))\tilde{M}^{-1}_{R,j,i}(\tilde{e}_{j,i}(t)) \end{bmatrix}$$
$$,\text{for } i \in \mathbb{N}_T,\ j \in \mathbb{N}_{F_i}$$

$$\tilde{D}_{j,i}(\tilde{e}_{j,i}(t)) = \begin{bmatrix} B_{r,j,i} & 0 \\ S_9 & S_{10} \end{bmatrix}, \text{for } i \in \mathbb{N}_T,\ j \in \mathbb{N}_{F_i}$$

$$\tilde{f}_{-j,i}(\tilde{e}_{j,i}(t)) = \begin{bmatrix} 0 \\ S_{10}f_{-j,i}(\tilde{e}_{j,i}(t)) \end{bmatrix}$$
$$,\text{for } i \in \mathbb{N}_T,\ j \in \mathbb{N}_{F_i}$$

$$S_9 = [0, [-S_6B_{r,j,i}]^T, 0]^T, S_{10} = diag(S_5, I)$$

where $\tilde{J}_{t,i}(\tilde{e}_{0,i}(t)) = J_{t,i}(\tilde{X}_{t,i}(t) + S_3X_{r,0,i}(t))$; $\tilde{M}_{t,i}(\tilde{e}_{0,i}(t)) = \bar{M}_{t,i}(\tilde{X}_{t,i}(t) + S_3X_{r,0,i}(t))$; $\tilde{H}_{t,i}(\tilde{e}_{0,i}(t)) =$

$\bar{H}_{t,i}(\tilde{X}_{t,i}(t){+}S_3X_{r,0,i}(t), \tilde{J}_{E,j,i}(\tilde{e}_{j,i}(t)) = J_{E,j,i}(S_5^{-1}\tilde{q}_{j,i}(t))$; $\tilde{G}_{j,i}(\tilde{e}_{j,i}(t)) = G_{j,i}(S_2(\tilde{X}_{R,j,i}(t){+}S_6X_{r,j,i}(t)), S_5^{-1}\tilde{q}_{j,i}(t))$; $\tilde{M}_{R,j,i}(\tilde{e}_{j,i}(t)) = M_{R,j,i}(S_5^{-1}\tilde{q}_{j,i}(t))$; $\tilde{H}_{R,j,i}(\tilde{e}_{j,i}(t)) = H_{R,j,i}(S_5^{-1}\tilde{q}_{j,i}(t), \tilde{J}_{E,j,i}(\tilde{e}_{j,i}(t))\mathcal{V}_{h,j,i}(t))$; $\tilde{B}_{t,i}(\tilde{e}_{0,i}(t)) = \bar{B}_{t,i}(\tilde{X}_{t,i}(t){+}S_3X_{r,0,i}(t))$; $f_{-0,i}(\tilde{e}_{0,i}(t)) = [f_{0,1,i}(X_{0,i}(t)), \cdots, f_{0,(i-1),i}(X_{0,i}(t)), f_{0,(i+1),i}(X_{0,i}(t)), \cdots, f_{0,N_T,i}(X_{0,i}(t))]$; $f_{-j,i}(\tilde{e}_{j,i}(t)) = [f_{j,0,i}(X_{j,i}(t)), \cdots, f_{j,(j-1),i}(X_{j,i}(t)), f_{j,(j+1),i}(X_{j,i}(t)), \cdots, f_{j,N_i,i}(X_{j,i}(t))]$; $X_{-0,i}(t) = [X_{0,1}^T(t), \cdots, X_{0,(i-1)}^T(t), X_{0,(i+1)}^T(t), \cdots, X_{0,N_T}^T(t)]^T \in \mathbb{R}^{n_{-x,0,i}}$; $X_{-j,i}(t) = [X_{0,i}^T(t), \cdots, X_{j-1,i}^T(t), X_{j+1,i}^T(t), \cdots, X_{N_i,i}^T(t)]^T \in \mathbb{R}^{n_{-x,j,i}}$. The corresponding index $n_{v,0,i} = n_{e,0,i}$, $n_{v,j,i} = n_{e,j,i}$, $n_{-x,0,i} = n_L \times (N_T - 1)$ and $n_{-x,j,i} = n_F \times (N_i - 1)$.

Subsequently, from the inverse dynamics in (13) and (22), the nominal actuator-torque can be exactly determined and regarded as the feed-forward control torque of each leader-follower hybrid team. Therefore, the control input $U_{0,i}(t)$ for the leader in the ith hybrid team and the control input $U_{j,i}(t)$ for the jth follower in the ith hybrid team can be partitioned into the feed-forward part and feedback part as follows:

$$U_{0,i}(t) = \tau_{inv,t,i}(t) + \tau_{fb,t,i}(t), \text{for } i \in \mathbb{N}_T \tag{46}$$

$$U_{j,i}(t) = \tau_{inv,R,j,i}(t) + \tau_{fb,R,j,i}(t) \quad ,\text{for } i \in \mathbb{N}_T,\ j \in \mathbb{N}_{F_i} \tag{47}$$

where $\tau_{inv,t,i}(t)$ is the nominal torque of the tractor-trailer (i.e., leader) in the ith hybrid team and $\tau_{inv,R,j,i}(t)$ is nominal torque of the jth biped robot (i.e., follower) in the ith hybrid team. These nominal control torques can be obtained from the computation of inverse dynamics in (13) and (22), respectively; $\tau_{fb,t,i}(t)$ and $\tau_{fb,R,j,i}(t)$ are the compensated feedback control torque for the tractor-trailer in the ith hybrid team and the jth biped robot in the ith hybrid team, respectively. In this situation, the feed-forward and feedback control mechanism can save the control effort efficiently [39] to improve the robustness of the augmented collaborative team formation tracking error dynamic system against the effects of unknown external disturbances and the wireless communication couplings.

For the convenience of design, the control inputs $\tau_{inv,t,i}(t)$ and $\tau_{fb,t,i}(t)$ in (46) for the the leader in the ith hybrid team and the control inputs $\tau_{inv,t,i}(t)$ and $\tau_{fb,t,i}(t)$ in (47) for the the jth follower in the ith hybrid team are specified as follows:

$$\tau_{inv,t,i}(t) = ID_{t,i}(\dot{\mathcal{V}}_{td,i}(t), \mathcal{V}_{t,i}(t), X_{t,i}(t)) \quad ,\text{for } i \in \mathbb{N}_T \tag{48}$$

$$\tau_{fb,t,i}(t) = \tilde{B}_{t,o,i}^{-1}(\tilde{e}_{0,i}(t))\tilde{M}_{t,o,i}(\tilde{e}_{0,i}(t))u_{0,i}(t) \quad ,\text{for } i \in \mathbb{N}_T \tag{49}$$

$$\tau_{inv,R,j,i}(t) = ID_{R,j,i}(\dot{\mathcal{V}}_{hd,j,i}(t), \mathcal{V}_{h,j,i}(t), q_{j,i}(t)) \quad ,\text{for } i \in \mathbb{N}_T,\ j \in \mathbb{N}_{F_i} \tag{50}$$

$$\tau_{fb,R,j,i}(t) = \tilde{M}_{R,o,j,i}(\tilde{e}_{j,i}(t))\tilde{J}_{E,o,j,i}(\tilde{e}_{j,i}(t))u_{j,i}(t) \quad ,\text{for } i \in \mathbb{N}_T,\ j \in \mathbb{N}_{F_i} \tag{51}$$

with

$$\begin{aligned}
&\dot{\mathcal{V}}_{hd,j,i}(t) = S_{11}a_{d,j,i}(\tilde{e}_{j,i}(t)),\\
&\mathcal{V}_{h,j,i}(t) = \tilde{G}_{j,i}^{\dagger}(\tilde{e}_{j,i}(t))\dot{X}_{j,i}(t),\\
&a_{d,j,i}(\tilde{e}_{j,i}(t)) = diag(I_8, [\tilde{J}_{bo,j,i}^{-1}(\tilde{e}_{j,i}(t)), \dot{\tilde{J}}_{bo,j,i}^{-1}(\tilde{e}_{j,i}(t))])\\
&\qquad \times \bar{G}_{j,i}^{\dagger}(\tilde{e}_{j,i}(t))[\dot{X}_{d,j,i}^T(t), \ddot{X}_{d,j,i}^T(t)]^T,\\
&\bar{G}_{j,i}^{\dagger}(\tilde{e}_{j,i}(t)) = diag([\tilde{G}_{j,i}^{\dagger}(\tilde{e}_{j,i}(t)), \tilde{G}_{j,i}^{\dagger}(\tilde{e}_{j,i}(t))]^T\\
&\qquad , \tilde{G}_{j,i}^{\dagger}(\tilde{e}_{j,i}(t))),\\
&\tilde{G}_{j,i}^{\dagger}(\tilde{e}_{j,i}(t)) = G_{j,i}^{\dagger}(S_2(\tilde{X}_{R,j,i}(t) + S_6X_{r,j,i}(t))\\
&\qquad , S_5^{-1}\tilde{q}_{j,i}(t)),\\
&S_{11} = diag(I_8, S_{12}), S_{12} = [0_{4\times 2}, -I_4[0_2, -I_2]^T]
\end{aligned}$$

where $u_{0,i}(t)$ and $u_{j,i}(t)$ are the feedback control input of the leader in the ith hybrid team and the jth follower in the ith hybrid team, respectively. $ID_{t,i}(\cdot,\cdot,\cdot)$ is the inverse dynamics of tractor-trailer in the ith hybrid team, whose desired linear acceleration $\dot{\mathcal{V}}_{td,i}(t)$ can be obtained from the reference model of leader in (27). $ID_{R,j,i}(\cdot,\cdot,\cdot)$ is the inverse dynamics of the jth biped robot in the ith hybrid team; $a_{d,j,i}(\cdot)$ is the desired acceleration of the jth biped robot leg motions in the ith hybrid team, which is obtained from the desired planar acceleration $\ddot{X}_{d,j,i}(t)$ and desired planar velocity $\dot{X}_{d,j,i}(t)$ in (28). $G_{j,i}^{\dagger}(\cdot,\cdot)$ is the right inverse of the linear transformation mapping $G_{j,i}(\cdot,\cdot)$ (i.e., the composite function $(G_{j,i} \circ G_{j,i}^{\dagger})(\cdot,\cdot) = I_3$) of the jth biped robot in the ith hybrid team; $\tilde{M}_{t,o,i}(\tilde{e}_{0,i}(t)) = \bar{M}_{t,o,i}(\tilde{X}_{t,i}(t) + S_3X_{r,0,i}(t))$ is the nominal dynamic system matrix of the tractor-trailer in the ith hybrid team; $\tilde{B}_{t,o,i}^{-1}(\tilde{e}_{0,i}(t)) = \bar{B}_{t,o,i}^{-1}(\tilde{X}_{t,i}(t) + S_3X_{r,0,i}(t))$ is the inverse of input transformation matrices of the tractor-trailer in the ith hybrid team; $\tilde{M}_{R,o,j,i}(\tilde{e}_{j,i}(t)) = M_{R,o,j,i}(S_5^{-1}\tilde{q}_{j,i}(t))$ is the nominal dynamic system matrix of the jth biped robot in the ith hybrid team; $\tilde{J}_{E,o,j,i}(\tilde{e}_{j,i}(t)) = J_{E,o,j,i}(S_5^{-1}\tilde{q}_{j,i}(t))$ and $\tilde{J}_{b,o,j,i}(\tilde{e}_{j,i}(t)) = J_{b,o,j,i}(S_1S_5^{-1}\tilde{q}_{j,i}(t))$ are the inverses of the nominal Jacobian functions of the jth biped robot in the ith hybrid team.

By substituting the proposed controller strategy in (46) and (47) into the augmented collaborative team formation tracking error dynamic system in (45), the augmented collaborative team formation tracking error dynamic system of the jth leader-follower team formation subsystem in the ith hybrid team can be reformulated as follows:

$$\begin{aligned}
\dot{\tilde{e}}_{j,i}(t) = {} & [\tilde{f}_{o,j,i}(\tilde{e}_{j,i}(t)) + \triangle\tilde{f}_{j,i}(\tilde{e}_{j,i}(t))] + [\tilde{g}_{o,j,i}\\
& + \triangle\tilde{g}_{j,i}(\tilde{e}_{j,i}(t))]u_{j,i}(t) + \tilde{D}(\tilde{e}_{j,i}(t))\tilde{v}_{j,i}(t)\\
& + \tilde{f}_{-j,i}(\tilde{e}_{j,i}(t))\tilde{X}_{-j,i}(t), \text{for } i \in \mathbb{N}_T,\ j \in \mathbb{N}_i
\end{aligned} \tag{52}$$

with the following dynamic functions:

$$\tilde{f}_{o,0,i}(\tilde{e}_{0,i}(t)) = \begin{bmatrix} A_{r,0,i}X_{r,0,i}(t) \\ \tilde{J}_{t,o,i}(\tilde{e}_{0,i}(t))[\tilde{\mathcal{V}}_{t,i}(t) \\ +S_4X_{r,0,i}(t)] \\ -S_3A_{r,0,i}X_{r,0,i}(t) \\ \dot{\mathcal{V}}_{td,i}(t) - S_4A_{r,0,i}X_{r,0,i}(t) \end{bmatrix} \quad ,\text{for } i \in \mathbb{N}_T$$

$$\triangle\tilde{f}_{0,i}(\tilde{e}_{0,i}(t)) = \begin{bmatrix} 0 \\ [\tilde{J}_{t,i}(\tilde{e}_{0,i}(t)) - \tilde{J}_{t,o}(\tilde{e}_{0,i}(t))]\times \\ [\tilde{\mathcal{V}}_{t,i}(t) + S_4 X_{r,0,i}(t)] \\ \tilde{M}_{t,i}^{-1}(\tilde{e}_{0,i}(t))\{[\tilde{B}_{t,i}(\tilde{e}_{0,i}(t)) \\ \times\tilde{B}_{t,o}^{-1}(\tilde{e}_{0,i}(t))\tilde{H}_{t,o,i}(\tilde{e}_{0,i}(t)) \\ -\tilde{H}_{t,i}(\tilde{e}_{0,i}(t))] + [\tilde{B}_{t,i}(\tilde{e}_{0,i}(t)) \\ \times\tilde{B}_{t,o}^{-1}(\tilde{e}_{0,i}(t))\tilde{M}_{t,o,i}(\tilde{e}_{0,i}(t)) \\ -\tilde{M}_{t,i}(\tilde{e}_{0,i}(t))]\dot{\mathcal{V}}_{td,i}(t)\} \end{bmatrix}$$
$$, \text{for } i \in \mathbb{N}_T$$

$$\triangle\tilde{g}_{0,i}(\tilde{e}_{0,i}(t)) = \begin{bmatrix} 0 \\ \tilde{M}_{t,i}^{-1}(\tilde{e}_{0,i}(t))\tilde{B}_{t,i}(\tilde{e}_{0,i}(t)) \\ \times[\tilde{B}_{t,o,i}^{-1}(\tilde{e}_{0,i}(t))\tilde{M}_{t,o,i}(\tilde{e}_{0,i}(t)) \\ -\tilde{B}_{t,i}^{-1}(\tilde{e}_{0,i}(t))\tilde{M}_{t,i}(\tilde{e}_{0,i}(t))] \end{bmatrix}$$
$$, \text{for } i \in \mathbb{N}_T$$

$$\tilde{f}_{o,j,i}(\tilde{e}_{j,i}(t)) = \begin{bmatrix} A_{r,j,i}X_{r,j,i}(t) \\ S_5\tilde{J}_{E,o,j,i}(\tilde{e}_{j,i}(t))\mathcal{V}_{h,j,i}(t) \\ \tilde{G}_{j,i}(\tilde{e}_{j,i}(t))S_1\mathcal{V}_{h,j,i}(t) \\ -S_6A_{r,j,i}X_{r,j,i}(t) \\ \dot{\mathcal{V}}_{hd,j,i}(t) \end{bmatrix}$$
$$, \text{for } i \in \mathbb{N}_T,\ j \in \mathbb{N}_{F_i}$$

$$\triangle\tilde{f}_{j,i}(\tilde{e}_{j,i}(t)) = \begin{bmatrix} S_5[\tilde{J}_{E,j,i}(\tilde{e}_{j,i}(t)) \\ -\tilde{J}_{E,o,j,i}(\tilde{e}_{j,i}(t))]\mathcal{V}_{h,j,i}(t) \\ 0 \\ \tilde{J}_{E,j,i}^{-1}(\tilde{e}_{j,i}(t))\tilde{M}_{R,j,i}^{-1}(\tilde{e}_{j,i}(t)) \\ \times\{[\tilde{H}_{R,o,j,i}(\tilde{e}_{j,i}(t)) \\ -\tilde{H}_{R,j,i}(\tilde{e}_{j,i}(t))] \\ +[\tilde{M}_{R,o,j,i}(\tilde{e}_{j,i}(t)) \\ \times\dot{\tilde{J}}_{E,o,j,i}(\tilde{e}_{j,i}(t))\mathcal{V}_{hd,j,i}(t) \\ -\tilde{M}_{R,j,i}(\tilde{e}_{j,i}(t))\dot{\tilde{J}}_{E,j,i}(\tilde{e}_{j,i}(t)) \\ \times\mathcal{V}_{h,j,i}(t)] + [\tilde{M}_{R,o,j,i}(\tilde{e}_{j,i}(t)) \\ \times\tilde{J}_{E,o,j,i}(\tilde{e}_{j,i}(t)) - \tilde{M}_{R,j,i}(\tilde{e}_{j,i}(t)) \\ \times\tilde{J}_{E,j,i}(\tilde{e}_{j,i}(t))]\dot{\mathcal{V}}_{hd,j,i}(t)\} \end{bmatrix}$$
$$, \text{for } i \in \mathbb{N}_T,\ j \in \mathbb{N}_{F_i}$$

$$\triangle\tilde{g}_{j,i}(\tilde{e}_{j,i}(t)) = \begin{bmatrix} 0 \\ \tilde{J}_{E,j,i}^{-1}(\tilde{e}_{j,i}(t))\tilde{M}_{R,j,i}^{-1}(\tilde{e}_{j,i}(t)) \\ \times[\tilde{M}_{R,o,j,i}(\tilde{e}_{j,i}(t))\tilde{J}_{E,o,j,i}(\tilde{e}_{j,i}(t)) \\ -\tilde{M}_{R,j,i}(\tilde{e}_{j,i}(t))\tilde{J}_{E,j,i}(\tilde{e}_{j,i}(t))] \end{bmatrix}$$
$$, \text{for } i \in \mathbb{N}_T,\ j \in \mathbb{N}_{F_i}$$

$$\tilde{g}_{o,0,i} = \begin{bmatrix} 0 \\ I_2 \end{bmatrix}, \text{for } i \in \mathbb{N}_T$$
$$\tilde{g}_{o,j,i} = \begin{bmatrix} 0 \\ I_{12} \end{bmatrix}, \text{for } i \in \mathbb{N}_T,\ j \in \mathbb{N}_{F_i}$$

where $\triangle\tilde{f}_{0,i}(\tilde{e}_{0,i}(t))$ and $\triangle\tilde{g}_{0,i}(\tilde{e}_{0,i}(t))$ represent the difference between the true and nominal dynamic functions for the leader in the ith hybrid team, $\triangle\tilde{f}_{j,i}(\tilde{e}_{j,i}(t))$ and $\triangle\tilde{g}_{j,i}(\tilde{e}_{j,i}(t))$ represent the difference between the true and nominal dynamic models.

As a result, by utilizing the augmented collaborative team formation tracking error dynamic system in (52), the robust H_∞ decentralized collaborative team formation tracking control strategy for the leader in the ith hybrid team in (41) and the jth follower in the ith hybrid team in (42) can be merged in and reformulated as follows:

$$J_{\infty,j,i}(u_{j,i}(t)) = \sup_{\substack{\tilde{v}_{j,i}(t),\\ \tilde{X}_{-j,i}(t)}} \frac{\int_0^{t_f}[\tilde{e}_{j,i}^T(t)\tilde{Q}_{j,i}\tilde{e}_{j,i}(t) + u_{j,i}^T(t)R_{j,i}u_{j,i}(t)]dt - V_{e,j,i}(\tilde{e}_{j,i}(0))}{\int_0^{t_f}[\tilde{v}_{j,i}^T(t)\tilde{v}_{j,i}(t) + \tilde{X}_{-j,i}^T(t)\tilde{X}_{-j,i}(t)]dt} \leq \rho_{j,i}^2 \tag{53}$$
$$, \text{for } i \in \mathbb{N}_T,\ j \in \mathbb{N}_i$$

with the following augmented weighting matrics:

$$\tilde{Q}_{0,i} = diag(0, Q_{1,0,i}, Q_{2,0,i}), \text{for } i \in \mathbb{N}_T$$
$$\tilde{Q}_{j,i} = diag(0, \bar{Q}_{1,j,i}, Q_{2,j,i}, 0), \text{for } i \in \mathbb{N}_T,\ j \in \mathbb{N}_{F_i}$$

where $V_{e,j,i}(\tilde{e}_{j,i}(0))$ is the energy of initial condition of the augmented collaborative team formation tracking error dynamic system with $V_{e,j,i}(\cdot) > 0$ and $V_{e,j,i}(\cdot) \in C^2(\mathbb{R}^{n_{e,j,i}})$. In conclusion, in this study, the main purpose of the robust H_∞ decentralized collaborative team formation tracking control strategy in (53) is to specify the control input $u_{j,i}(t)$ to attenuate the effect of any finite energy external disturbances and couplings on the team formation tracking and control strategy of each leader-follower hybrid team under the prescribed attenuation level $\rho_{j,i}^2 > 0$. Once the control input $u_{j,i}(t)$ is specified such that the objective $J_{\infty,j,i}(u_{j,i}(t)) \leq \rho_{j,i}^2$ is achieved, the effect of external disturbance $\tilde{v}_{j,i}(t)$ and wireless interference $\tilde{X}_{-j,i}(t)$ on the collaborative team formation tracking performance can be guaranteed below the prescribed attenuation level $\rho_{j,i}^2$ for each leader-follower hybrid team. Moreover, if the effect of external disturbance $\tilde{v}_{j,i}(t)$ and wireless interference $\tilde{X}_{-j,i}(t)$ are vanished (i.e., $\tilde{v}_{j,i}(t) = 0$, $\tilde{X}_{-j,i}(t) = 0$ and $\rho_{j,i}^2 = \infty$), at this situation, we will prove that the following asymptotic H_2 quadratic tracking performance of the desired collaborative team formation can be achieved by the proposed robust H_∞ decentralized collaborative team formation tracking control strategy with $\rho_{j,i}^2 = \infty$ [50], [51]:

$$\int_0^{t_f}[\tilde{e}_{j,i}^T(t)\tilde{Q}_{j,i}\tilde{e}_{j,i}(t) + u_{j,i}^T(t)R_{j,i}u_{j,i}(t)]dt \leq V_{e,j,i}(\tilde{e}_{j,i}(0)), \forall t_f \in [0,\infty], \text{for } i \in \mathbb{N}_T, j \in \mathbb{N}_i \tag{54}$$

i.e., $V_{e,j,i}(\tilde{e}_{j,i}(0))$ is the upper bound of the H_2 quadratic tracking performance. We can also achieve the optimal H_2 quadratic tracking control by minimizing its upper bound $V_{e,j,i}(\tilde{e}_{j,i}(0))$.

Before coming into the design of robust H_∞ decentralized collaborative team formation tracking control in (53), the following assumption and lemma are provided.

Assumption IV.1: There exist known bounding matrices $\triangle F_{j,i} \in \mathbb{R}^{n_{e,j,i}\times n_{e,j,i}}$ and scalar $\triangle\varepsilon_{j,i} \in \mathbb{R} \geq 0$ for $i \in \mathbb{N}_T$, $j \in \mathbb{N}_i$, such that:

$$\left\|\triangle\tilde{f}_{j,i}(\tilde{e}_{j,i}(t))\right\| \leq \|\triangle F_{j,i}\tilde{e}_{j,i}(t)\|, \text{for } i \in \mathbb{N}_T, j \in \mathbb{N}_i$$
$$\|\triangle\tilde{g}_{j,i}(\tilde{e}_{j,i}(t))\| \leq \triangle\varepsilon_{j,i}, \text{for } i \in \mathbb{N}_T, j \in \mathbb{N}_i \tag{55}$$

Lemma 1: ([45]) For any matrix X and Y with appropriate dimensions, the following inequality holds:

$$X^TY + Y^TX \leq X^TP^{-1}X + Y^TPY \quad (56)$$

where P is any positive definite symmetric matrix.

Theorem 1: For the augmented collaborative team formation tracking error dynamic system in (52), considering the differentiable Lyapunov function $V_{e,j,i}(\tilde{e}_{j,i}(t))$, for $i \in \mathbb{N}_T$, $j \in \mathbb{N}_i$, if the following HJI has a positive solution $V_{e,j,i}(\tilde{e}_{j,i}(t)) > 0$ for each leader-follower hybrid team

$$\begin{aligned}
&\tilde{e}_{j,i}^T(t)[\tilde{Q}_{j,i} + \triangle F_{j,i}^T\triangle F_{j,i}]\tilde{e}_{j,i}(t)\\
&+u_{j,i}^T(t)[R_{j,i} + (\triangle\varepsilon_{j,i})^2 I]u_{j,i}(t)\\
&+(\tfrac{\partial V_{e,j,i}(\tilde{e}_{j,i}(t))}{\partial \tilde{e}_{j,i}(t)})^T[\tilde{f}_{o,j,i}(\tilde{e}_{j,i}(t)) + \tilde{g}_{o,j,i}u_{j,i}(t)]\\
&+\tfrac{1}{2}(\tfrac{\partial V_{e,j,i}(\tilde{e}_{j,i}(t))}{\partial \tilde{e}_{j,i}(t)})^T\tfrac{\partial V_{e,j,i}(\tilde{e}_{j,i}(t))}{\partial \tilde{e}_{j,i}(t)}\\
&+\tfrac{1}{4\rho_{j,i}^2}(\tfrac{\partial V_{e,j,i}(\tilde{e}_{j,i}(t))}{\partial \tilde{e}_{j,i}(t)})^T\tilde{D}(\tilde{e}_{j,i}(t))\\
&\times\tilde{D}(\tilde{e}_{j,i}(t))^T\tfrac{\partial V_{e,j,i}(\tilde{e}_{j,i}(t))}{\partial \tilde{e}_{j,i}(t)}\\
&+\tfrac{1}{4\rho_{j,i}^2}(\tfrac{\partial V_{e,j,i}(\tilde{e}_{j,i}(t))}{\partial \tilde{e}_{j,i}(t)})^T\tilde{f}_{-j,i}(\tilde{e}_{j,i}(t))\\
&\times\tilde{f}_{-j,i}^T(\tilde{e}_{j,i}(t))\tfrac{\partial V_{e,j,i}(\tilde{e}_{j,i}(t))}{\partial \tilde{e}_{j,i}(t)}\\
&< 0, \text{for } i \in \mathbb{N}_T,\ j \in \mathbb{N}_i
\end{aligned} \quad (57)$$

then the jth leader-follower team formation subsystem in the ith hybrid team achieve robust H_∞ decentralized collaborative team formation tracking performance with a prescribed attenuation level $\rho_{j,i}^2$ in (53). Moreover, if the external disturbance and wireless communication couplings in (52) are vanished (i.e., $\tilde{v}_{j,i}(t) = 0$ and $\tilde{X}_{-j,i}(t) = 0$), the H_2 asymptotically collaborative team formation tracking performance in (54) can be achieved, i.e., $\tilde{e}_{j,i}(t) \to 0$, for $i \in \mathbb{N}_T$, $j \in \mathbb{N}_i$, as $t \to \infty$.

Proof. From the time integral part in the numerator of H_∞ performance index in (53) and by chain rule, we get

$$\begin{aligned}
&\textstyle\int_0^{t_f}[\tilde{e}_{j,i}^T(t)\tilde{Q}_{j,i}\tilde{e}_{j,i}(t) + u_{j,i}^T(t)R_{j,i}u_{j,i}(t)]dt\\
&= \textstyle\int_0^{t_f}[\tilde{e}_{j,i}^T(t)\tilde{Q}_{j,i}\tilde{e}_{j,i}(t) + u_{j,i}^T(t)R_{j,i}u_{j,i}(t)\\
&+\tfrac{dV_{e,j,i}(\tilde{e}_{j,i}(t))}{dt}]dt + V_{e,j,i}(\tilde{e}_{j,i}(0)) - V_{e,j,i}(\tilde{e}_{j,i}(t_f))\\
&\leq \textstyle\int_0^{t_f}[\tilde{e}_{j,i}^T(t)\tilde{Q}_{j,i}\tilde{e}_{j,i}(t) + u_{j,i}^T(t)R_{j,i}u_{j,i}(t)\\
&+(\tfrac{\partial V_{e,j,i}(\tilde{e}_{j,i}(t))}{\partial \tilde{e}_{j,i}(t)})^T\{[\tilde{f}_{o,j,i}(\tilde{e}_{j,i}(t)) + \triangle\tilde{f}_{j,i}(\tilde{e}_{j,i}(t))]\\
&+\left[\tilde{g}_{o,j,i} + \triangle\tilde{g}_{j,i}(\tilde{e}_{j,i}(t))\right]\tilde{u}_{j,i}(t) + \tilde{D}(\tilde{e}_{j,i}(t))\tilde{v}_{j,i}(t)\\
&+\tilde{f}_{-j,i}(\tilde{e}_{j,i}(t))\tilde{X}_{-j,i}(t)\}dt + V_{e,j,i}(\tilde{e}_{j,i}(0))
\end{aligned} \quad (58)$$

By Lemma 1, with $P = \frac{1}{2}I$, we get

$$\begin{aligned}
&\textstyle\int_0^{t_f}\{(\tfrac{\partial V_{e,j,i}(\tilde{e}_{j,i}(t))}{\partial \tilde{e}_{j,i}(t)})^T[\triangle\tilde{f}_{j,i}(\tilde{e}_{j,i}(t))\\
&+\triangle\tilde{g}_{j,i}(\tilde{e}_{j,i}(t))u_{j,i}(t)]\}dt\\
&\leq \textstyle\int_0^{t_f}[\tfrac{1}{2}(\tfrac{\partial V_{e,j,i}(\tilde{e}_{j,i}(t))}{\partial \tilde{e}_{j,i}(t)})^T\tfrac{\partial V_{e,j,i}(\tilde{e}_{j,i}(t))}{\partial \tilde{e}_{j,i}(t)}\\
&+\triangle\tilde{f}_{j,i}(\tilde{e}_{j,i}(t))^T\triangle\tilde{f}_{j,i}(\tilde{e}_{j,i}(t))\\
&+u_{j,i}^T(t)\triangle\tilde{g}_{j,i}^T(\tilde{e}_{j,i}(t))\triangle\tilde{g}_{j,i}(\tilde{e}_{j,i}(t))u_{j,i}(t)]dt
\end{aligned} \quad (59)$$

In addition, also by Lemma 1, with $P = \frac{1}{2\rho_{j,i}^2}I$, we obtain

$$\begin{aligned}
&\textstyle\int_0^{t_f}[(\tfrac{\partial V_{e,j,i}(\tilde{e}_{j,i}(t))}{\partial \tilde{e}_{j,i}(t)})^T(\tilde{D}(\tilde{e}_{j,i}(t))\tilde{v}_{j,i}(t)\\
&+\tilde{f}_{-j,i}(\tilde{e}_{j,i}(t))\tilde{X}_{-j,i}(t)]dt\\
&\leq \textstyle\int_0^{t_f}[\tfrac{1}{4\rho_{j,i}^2}(\tfrac{\partial V_{e,j,i}(\tilde{e}_{j,i}(t))}{\partial \tilde{e}_{j,i}(t)})^T\tilde{f}_{-j,i}(\tilde{e}_{j,i}(t))\\
&\times\tilde{f}_{-j,i}^T(\tilde{e}_{j,i}(t))\tfrac{\partial V_{e,j,i}(\tilde{e}_{j,i}(t))}{\partial \tilde{e}_{j,i}(t)}\\
&+\tfrac{1}{4\rho_{j,i}^2}(\tfrac{\partial V_{e,j,i}(\tilde{e}_{j,i}(t))}{\partial \tilde{e}_{j,i}(t)})^T\tilde{D}(\tilde{e}_{j,i}(t))\\
&\times\tilde{D}(\tilde{e}_{j,i}(t))^T\tfrac{\partial V_{e,j,i}(\tilde{e}_{j,i}(t))}{\partial \tilde{e}_{j,i}(t)}\\
&+\rho_{j,i}^2\tilde{v}_{j,i}^T(t)\tilde{v}_{j,i}(t) + \rho_{j,i}^2\tilde{X}_{-j,i}^T(t)\tilde{X}_{-j,i}(t)]dt
\end{aligned} \quad (60)$$

Based on the *Assumption IV.1,* we can get

$$\begin{aligned}
&\textstyle\int_0^{t_f}[\triangle\tilde{f}_{j,i}(\tilde{e}_{j,i}(t))^T\triangle\tilde{f}_{j,i}(\tilde{e}_{j,i}(t))\\
&+u_{j,i}^T(t)\triangle\tilde{g}_{j,i}^T(\tilde{e}_{j,i}(t))\triangle\tilde{g}_{j,i}(\tilde{e}_{j,i}(t))u_{j,i}(t)]dt\\
&< \textstyle\int_0^{t_f}\{\tilde{e}_{j,i}^T(t)\triangle F_{j,i}^T\triangle F_{j,i}\tilde{e}_{j,i}(t)\\
&+(\triangle\varepsilon_{j,i})^2 u_{j,i}^T(t)u_{j,i}(t)\}dt
\end{aligned} \quad (61)$$

Therefore, by (58) - (61), we obtain

$$\begin{aligned}
&\textstyle\int_0^{t_f}[\tilde{e}_{j,i}^T(t)\tilde{Q}_{j,i}\tilde{e}_{j,i}(t) + u_{j,i}^T(t)R_{j,i}u_{j,i}(t)]dt\\
&\leq \textstyle\int_0^{t_f}(\tilde{e}_{j,i}^T(t)[\tilde{Q}_{j,i} + \triangle F_{j,i}^T\triangle F_{j,i}]\tilde{e}_{j,i}(t)\\
&+u_{j,i}^T(t)[R_{j,i} + (\triangle\varepsilon_{j,i})^2 I]u_{j,i}(t)\\
&+(\tfrac{\partial V_{e,j,i}(\tilde{e}_{j,i}(t))}{\partial \tilde{e}_{j,i}(t)})^T[\tilde{f}_{o,j,i}(\tilde{e}_{j,i}(t)) + \tilde{g}_{o,j,i}u_{j,i}(t)]\\
&+\tfrac{1}{2}(\tfrac{\partial V_{e,j,i}(\tilde{e}_{j,i}(t))}{\partial \tilde{e}_{j,i}(t)})^T\tfrac{\partial V_{e,j,i}(\tilde{e}_{j,i}(t))}{\partial \tilde{e}_{j,i}(t)}\\
&+\tfrac{1}{4\rho_{j,i}^2}(\tfrac{\partial V_{e,j,i}(\tilde{e}_{j,i}(t))}{\partial \tilde{e}_{j,i}(t)})^T\tilde{D}(\tilde{e}_{j,i}(t))\\
&\times\tilde{D}(\tilde{e}_{j,i}(t))^T\tfrac{\partial V_{e,j,i}(\tilde{e}_{j,i}(t))}{\partial \tilde{e}_{j,i}(t)} + \tfrac{1}{4\rho_{j,i}^2}(\tfrac{\partial V_{e,j,i}(\tilde{e}_{j,i}(t))}{\partial \tilde{e}_{j,i}(t)})^T\\
&\times\tilde{f}_{-j,i}(\tilde{e}_{j,i}(t))\tilde{f}_{-j,i}^T(\tilde{e}_{j,i}(t))\tfrac{\partial V_{e,j,i}(\tilde{e}_{j,i}(t))}{\partial \tilde{e}_{j,i}(t)}\\
&+\rho_{j,i}^2\tilde{v}_{j,i}^T(t)\tilde{v}_{j,i}(t) + \rho_{j,i}^2\tilde{X}_{-j,i}^T(t)\tilde{X}_{-j,i}(t))dt\\
&+V_{e,j,i}(\tilde{e}_{j,i}(0))
\end{aligned}$$

If HJI in (57) holds, then the following inequality holds:

$$\begin{aligned}
&\textstyle\int_0^{t_f}[\tilde{e}_{j,i}^T(t)\tilde{Q}_{j,i}\tilde{e}_{j,i}(t) + u_{j,i}^T(t)R_{j,i}u_{j,i}(t)]dt\\
&\leq V_{e,j,i}(\tilde{e}_{j,i}(0)) + \rho_{j,i}^2\textstyle\int_0^{t_f}[\tilde{v}_{j,i}^T(t)\tilde{v}_{j,i}(t)\\
&+\tilde{X}_{-j,i}^T(t)\tilde{X}_{-j,i}(t)]dt, \text{for } i \in \mathbb{N}_T,\ j \in \mathbb{N}_i
\end{aligned} \quad (62)$$

which implies that

$$\frac{\begin{aligned}&\textstyle\int_0^{t_f}[\tilde{e}_{j,i}^T(t)\tilde{Q}_{j,i}\tilde{e}_{j,i}(t)\\&+u_{j,i}^T(t)R_{j,i}u_{j,i}(t)]dt\\&-V_{e,j,i}(\tilde{e}_{j,i}(0))\end{aligned}}{\begin{aligned}&\textstyle\int_0^{t_f}[\tilde{v}_{j,i}^T(t)\tilde{v}_{j,i}(t)\\&+\tilde{X}_{-j,i}^T(t)\tilde{X}_{-j,i}(t)]dt\end{aligned}} \leq \rho_{j,i}^2, \text{for } i \in \mathbb{N}_T,\ j \in \mathbb{N}_i$$

Accordingly, the robust H_∞ decentralized tracking control performance for the jth leader-follower team formation subsystem in the ith hybrid team in (53) is guaranteed with a prescribed disturbance attenuation level $\rho_{j,i}^2$.

On the other hand, if the external disturbance and the wireless communication couplings of each leader-follower hybrid team are vanished, that is, $\tilde{v}_{j,i}(t) = 0$ and $\tilde{X}_{-j,i}(t) = 0$, the inequalities in (62) can be written in the bounded H_2 collaborative team formation tracking control design problem in (54).

From (54), the total energy of the jth leader-follower team formation subsystem in the ith hybrid team on the time interval $[0,\infty]$ is bounded by the finite initial energy $V_{e,j,i}(\tilde{e}_{j,i}(0))$. As a result, as $t_f \to \infty$, the energy of the error dynamic state $\tilde{e}_{j,i}(t)$ will converge to zero, i.e., H_2 collaborative asymptotical team formation tracking performance. The proof is completed. ■

Remark 3: The robust H_∞ decentralized team formation tracking control design problem in (53) can be reduced to the H_2 decentralized team formation tracking control design problem in (54) if $\tilde{v}_{j,i}(t)=0$ and $\tilde{X}_{-j,i}(t)=0$ in (52) and $\rho_{j,i}^2=\infty$ in (53). For H_2 decentralized team formation tracking control design problem in (54), considering the differentiable Lyapunov function $V_{e,j,i}(\tilde{e}_{j,i}(t))$, for $i\in\mathbb{N}_T,\ j\in\mathbb{N}_i$, if the following HJI has a positive solution $V_{e,j,i}(\tilde{e}_{j,i}(t))>0$ for each leader-follower subsystem of the ith hybrid team [50]

$$\begin{aligned}&\tilde{e}_{j,i}^T(t)[\tilde{Q}_{j,i}+\triangle F_{j,i}^T\triangle F_{j,i}]\tilde{e}_{j,i}(t)+u_{j,i}^T(t)[R_{j,i}\\&+(\triangle\varepsilon_{j,i})^2 I]u_{j,i}(t)+(\tfrac{\partial V_{e,j,i}(\tilde{e}_{j,i}(t))}{\partial\tilde{e}_{j,i}(t)})^T\\&\times[\tilde{f}_{o,j,i}(\tilde{e}_{j,i}(t))+\tilde{g}_{o,j,i}u_{j,i}(t)]\\&+\tfrac{1}{2}(\tfrac{\partial V_{e,j,i}(\tilde{e}_{j,i}(t))}{\partial\tilde{e}_{j,i}(t)})^T\tfrac{\partial V_{e,j,i}(\tilde{e}_{j,i}(t))}{\partial\tilde{e}_{j,i}(t)}<0\\&,\text{for } i\in\mathbb{N}_T,\ j\in\mathbb{N}_i\end{aligned}\tag{63}$$

then the jth leader-follower team formation subsystem in the ith hybrid team can achieve the optimal H_2 decentralized collaborative team formation tracking performance in (54) by minimizing its upper bound [50], [51]:

$$\begin{aligned}&\min_{u_{j,i}(t)} V_{e,j,i}(\tilde{e}_{j,i}(0))\\&\text{subject to HJI in (63)}\end{aligned}\tag{64}$$

V. ROBUST H_∞ DECENTRALIZED COLLABORATIVE TEAM FORMATION TRACKING CONTROL DESIGN FOR HYBRID TEAMS OF TRACTOR-TRAILERS AND BIPED ROBOTS VIA NUMERICAL LPV MODELING APPROACH

To deal with the robust H_∞ decentralized collaborative team formation tracking control design problem in (53), the designer must solve the HJIs in (57). Unfortunately, the HJIs are too difficult to be solved in most cases, both analytically and numerically. Therefore, the tensor product (TP) model transformation is employed to approximate the augmented collaborative leader-follower team formation dynamic system in (52) efficiently such that the complicated HJIs in (57) can be transformed into a set of equivalent solvable LMIs which can be solved via MATLAB LMI TOOLBOX.

A. TENSOR PRODUCT MODEL TRANSFORMATION FOR AUGMENTED COLLABORATIVE LEADER-FOLLOWER TEAM FORMATION SUBSYSTEMS

In order to construct the LPV model of (52), to begin with, a closed hypercube $\Omega_{j,i}=[\alpha_{1,0,i},\beta_{1,0,i}]\times[\alpha_{2,0,i},\beta_{2,0,i}]\times\cdots\times[\alpha_{n_{e,j,i},0,i},\beta_{n_{e,j,i},0,i}]\subset\mathbb{R}^{n_{e,j,i}}$, for $i\in\mathbb{N}_T,\ j\in\mathbb{N}_i$ is defined and $\{\alpha_{m,j,i}\in\mathbb{R},\beta_{m,j,i}\in\mathbb{R}\}_{m=1}^{n_{e,j,i}}$. Subsequently, the set of sample points selected from $\Omega_{j,i}$ can be constructed as follows [34]- [37]:

$$\begin{aligned}&\Psi_{j,i}=\{[\alpha_1,\cdots,\alpha_{n_{e,j,i}}]^T||\alpha_1\in\{g_{l,1,j,i}\}_{l=1}^{M_{1,j,i}},\cdots\\&,\alpha_{n_e}\in\{g_{l,n_{e,j,i},j,i}\}_{l=1}^{M_{n_{e,j,i},j,i}}\},\text{for } i\in\mathbb{N}_T,\ j\in\mathbb{N}_i\end{aligned}\tag{65}$$

where $\{g_{l,m,j,i}\}_{l=1}^{M_{m,j,i}}$ are increasing sequence within the interval $[\alpha_{m,j,i},\beta_{m,j,i}]$, for $m\in\{1,\cdots,n_{e,j,i}\}$, i.e, $\alpha_{m,j,i}\le g_{1,m,j,i}<\cdots<g_{M_{m,j,i},m,j,i}\le\beta_{m,j,i}$. $M_{m,j,i}\in\mathbb{N}$ is the number of sample points for the mth elements in the jth augmented error dynamic state in the ith team in (43) or (44).

Subsequently, a three-dimensional sample data tensor $\mathcal{A}_{j,i}$ generated by sample data set $\Psi_{j,i}$ for the augmented collaborative team formation tracking error dynamic system of the jth leader-follower team formation subsystem in the ith hybrid team can be represented as follows:

$$\begin{aligned}\mathcal{A}_{j,i}=\{[&A_{k,j,i}=\tfrac{\partial\tilde{f}_{o,j,i}(\tilde{e}_{j,i}(t))}{\partial\tilde{e}_{j,i}(t)}|_{\tilde{e}_{j,i}(t)=\tilde{e}_{k,j,i}}\\&,D_{k,j,i}=\tilde{D}(\tilde{e}_{j,i}(t))|_{\tilde{e}_{j,i}(t)=\tilde{e}_{k,j,i}}\\&,\ A_{-k,j,i}=\tilde{f}_{-j,i}(\tilde{e}_{j,i}(t))|_{\tilde{e}_{j,i}(t)=\tilde{e}_{k,j,i}}]\\&||\forall\tilde{e}_{k,j,i}\in\Psi_{j,i}\}\\&,\text{for } i\in\mathbb{N}_T,\ j\in\mathbb{N}_i,k\in\{1,\cdots,M_{j,i}\}\end{aligned}\tag{66}$$

where $A_{k,j,i}\in\mathbb{R}^{n_{e,j,i}\times n_{e,j,i}}$, $D_{k,j,i}\in\mathbb{R}^{n_{e,j,i}\times n_{v,j,i}}$, and $A_{-k,j,i}\in\mathbb{R}^{n_{e,j,i}\times n_{-x,j,i}}$. In addition, from (66), it is clear that the sample data tenor $\mathcal{A}_{j,i}\in\mathbb{R}^{M_{j,i}\times n_{e,j,i}\times(n_{e,j,i}+n_{v,j,i}+n_{-x,j,i})}$ only collects the system matrices $A_{k,j,i}$, $D_{k,j,i}$, $A_{-k,j,i}$ of the jth leader-follower team formation subsystem in the ith hybrid team in (52) at sample points in $\Psi_{j,i}$, where $M_{j,i}=M_{1,j,i}+\cdots+M_{n_{e,j,i},j,i}$. Consequently, the corresponding Jacobian matrices can be derived by the numerical method when designers do not know the exact analytic expression of biped robot dynamics or tractor-trailer dynamics.

Afterwards, in order to extract the minimal basis of TP approximation, the reduced high-order singular value decomposition (RHOSVD) is to discard unimportant information in $\mathcal{A}_{j,i}$ (i.e., zero or smaller singular values and related singular vectors will be discarded) [34], [35]. Therefore, an extracted core tensor $\hat{\mathcal{S}}_{j,i}$ obtained by RHOSVD can be represented as follows:

$$\begin{aligned}&\hat{\mathcal{S}}_{j,i}=\{[\tilde{A}_{k,j,i},\tilde{D}_{k,j,i},\tilde{A}_{-k,j,i}]\}\\&,\text{for } i\in\mathbb{N}_T,\ j\in\mathbb{N}_i,k\in\{1,\cdots,L_{j,i}\}\end{aligned}\tag{67}$$

with

$$\begin{aligned}&\mathcal{A}_{j,i}\approx\hat{\mathcal{S}}_{j,i}\times_1\hat{H}_{j,i}\\&\hat{H}_{j,i}=\begin{bmatrix}h_{1,j,i}(\tilde{e}_{1,j,i}) & \cdots & h_{1,j,i}(\tilde{e}_{L_{j,i},j,i})\\ \vdots & \ddots & \vdots\\ h_{L_{j,i},j,i}(\tilde{e}_{1,j,i}) & \cdots & h_{L_{j,i},j,i}(\tilde{e}_{L_{j,i},j,i})\end{bmatrix}^T\\&,\text{for } i\in\mathbb{N}_T,\ j\in\mathbb{N}_i\end{aligned}$$

where $\tilde{A}_{k,j,i}\in\mathbb{R}^{n_{e,j,i}\times n_{e,j,i}}$, $\tilde{D}_{k,j,i}\in\mathbb{R}^{n_{e,j,i}\times n_{v,j,i}}$, and $\tilde{A}_{-k,j,i}\in\mathbb{R}^{n_{e,j,i}\times n_{-x,j,i}}$ are extracted system matrices; $\hat{H}_{j,i}\in\mathbb{R}^{L_{j,i}\times L_{j,i}}$ is the orthonormal basis matrix, which records the corresponding weights for the extracted core tensor $\hat{\mathcal{S}}_{j,i}$. $\times_n$denotes the n-mode product between a tensor and a matrix.

Accordingly, the augmented collaborative team formation tracking error dynamic system of the jth leader-follower team formation subsystem in the ith hybrid team in (52) can be approximated by the following LPV model:

$$\begin{aligned}\dot{\tilde{e}}_{j,i}(t) = \sum_{k=1}^{L_{j,i}} h_{k,j,i}(\tilde{e}_{j,i}(t))\{[\tilde{A}_{k,j,i}\tilde{e}_{j,i}(t) + \triangle\tilde{f}_{j,i}(\tilde{e}_{j,i}(t))] \\ + [\tilde{g}_{o,j,i} + \triangle\tilde{g}_{j,i}(\tilde{e}_{j,i}(t))]\, u_{j,i}(t) + \tilde{D}_{k,j,i}\tilde{v}_{j,i}(t) \\ + \tilde{A}_{-k,j,i}\tilde{X}_{-j,i}(t)\}, \text{for } i \in \mathbb{N}_T,\ j \in \mathbb{N}_i\end{aligned} \quad (68)$$

where $h_{k,j,i}(\cdot)$ is the weighting functions for interpolation of system matrices (i.e., $\tilde{A}_{k,j,i}$, $\tilde{D}_{k,j,i}$, $\tilde{A}_{-k,j,i}$), which satisfies the following properties:

$$(i)\ h_{k,j,i}(\tilde{e}_{j,i}(t)) \in [0,1], \forall k \in \{1,\cdots,L_{j,i}\}$$
$$(ii)\ \textstyle\sum_{k=1}^{L_{j,i}} h_{k,j,i}(\tilde{e}_{j,i}(t)) = 1, \forall \tilde{e}_{j,i}(t) \in \Omega_{j,i}$$

, i.e., each weighting function is non-negative and there exist at least one weighting function to be not zero during the interpolation, for $\tilde{e}_{j,i}(t) \in \Omega_{j,i}$.

Based on the LPV model in (68) and the corresponding weighting function properties, the decentralized collaborative team formation tracking control law $u_{j,i}(t)$ can be designed via the parallel distributed compensation (PDC) method as follows:

$$\begin{aligned}u_{j,i}(t) = \sum_{k=1}^{L_{j,i}} h_{k,j,i}(\tilde{e}_{j,i}(t))\tilde{K}_{k,j,i}\tilde{e}_{j,i}(t) \\ , \text{for } i \in \mathbb{N}_T,\ j \in \mathbb{N}_i\end{aligned} \quad (69)$$

where $\tilde{K}_{k,j,i} \in \mathbb{R}^{n_{u,j,i}\times n_{e,j,i}}$ is the control feedback gain, which will be designed later; $h_{k,j,i}(\cdot)$ is the interpolation weighting function in (68).

In addition, for the sake of simplicity, the full state information of the augmented collaborative team formation tracking error dynamic system is assumed to be directly accessed. As a result, by combining the augmented LPV model in (68) with the corresponding decentralized collaborative team formation tracking control in (69), the augmented collaborative team formation tracking error dynamic system of the jth leader-follower team formation subsystem in the ith hybrid team in (52) can be reformulated as follows:

$$\begin{aligned}\dot{\tilde{e}}_{j,i}(t) = \sum_{k=1}^{L_{j,i}} h_{k,j,i}(\tilde{e}_{j,i}(t))\{[\tilde{A}_{k,j,i}\tilde{e}_{j,i}(t) + \triangle\tilde{f}_{j,i}(\tilde{e}_{j,i}(t))] \\ + [\tilde{g}_{o,j,i} + \triangle\tilde{g}_{j,i}(\tilde{e}_{j,i}(t))]\, \tilde{K}_{k,j,i}\tilde{e}_{j,i}(t) \\ + \tilde{D}_{k,j,i}\tilde{v}_{j,i}(t) + \tilde{A}_{-k,j,i}\tilde{X}_{-j,i}(t)\} \\ , \text{for } i \in \mathbb{N}_T,\ j \in \mathbb{N}_i\end{aligned} \quad (70)$$

Remark 4: Conventionally, T-S fuzzy modeling method is also a powerful method to interpolate the nonlinear dynamic system by a set of local linear dynamic systems to simplify the complex HJI problems [46], [47]. However, most of time, the designers may not know the exact analytic expression of biped robot model or tractor-trailer model. In addition, it is not easy to choose the appropriate premise variables and the corresponding fuzzy set. Therefore, here we choose TP model transformation as an alternative and more convenient approach to construct the LPV model.

B. ROBUST H_∞ DECENTRALIZED COLLABORATIVE TEAM FORMATION TRACKING CONTROL DESIGN

To begin with, a differentiable Lyapunov function in the quadratic form is defined as follows:

$$V_{e,j,i}(\tilde{e}_{j,i}(t)) = \tilde{e}_{j,i}^T(t)P_{j,i}\tilde{e}_{j,i}(t), \text{for } i \in \mathbb{N}_T,\ j \in \mathbb{N}_i \quad (71)$$

where $P_{j,i} \in \mathbb{R}^{n_{e,j,i}\times n_{e,j,i}} > 0$ is a positive definite matrix.

Theorem 2: Consider the collaborative team formation tracking error dynamic system model in (70) with the quadratic Lyapunov function in (71), for $i \in \mathbb{N}_T,\ j \in \mathbb{N}_i$. The robust H_∞ decentralized collaborative team formation tracking strategy with a prescribed disturbance attenuation level $\rho_{j,i}^2$ in (53) can be achieved by the decentralized collaborative team formation tracking control law $u_{j,i}(t)$ in (69) if there exists the common solution $P_{j,i} = P_{j,i}^T > 0$ in the following Riccati-like inequalities:

$$\begin{aligned}&\tilde{Q}_{j,i} + \tilde{K}_{k,j,i}^T[\tilde{R}_{j,i} + (\triangle\varepsilon_{j,i})^2 I]\tilde{K}_{k,j,i} + P_{j,i}\tilde{A}_{k,j,i} \\ &+\tilde{A}_{k,j,i}^T P_{j,i} + P_{j,i}\tilde{g}_{o,j,i}\tilde{K}_{k,j,i} + \tilde{K}_{k,j,i}^T\tilde{g}_{o,j,i}^T P_{j,i} \\ &+2P_{j,i}P_{j,i} + \tfrac{1}{\rho_{j,i}^2}P_{j,i}\tilde{A}_{-k,j,i}\tilde{A}_{-k,j,i}^T P_{j,i} + \triangle F_{j,i}^T\triangle F_{j,i} \\ &+\tfrac{1}{\rho_{j,i}^2}P_{j,i}\tilde{D}_{k,j,i}\tilde{D}_{k,j,i}^T P_{j,i} < 0 \\ &, \text{for } i \in \mathbb{N}_T, j \in \mathbb{N}_i, k \in \{1,\cdots,L_{j,i}\}\end{aligned} \quad (72)$$

Furthermore, if the external disturbances and the couplings of the jth leader-follower team formation subsystem in the ith hybrid team are vanished (i.e., $\tilde{v}_{j,i}(t) = 0$ and $\tilde{X}_{-j,i}(t) = 0$), the H_2 quadratically asymptotical collaborative team formation tracking performance for the jth leader-follower team formation subsystem in the ith hybrid team in (54) can be achieved, i.e., $\tilde{e}_{j,i}(t) \to 0$, for $i \in \mathbb{N}_T, j \in \mathbb{N}_i$, as $t \to \infty$.

Proof. From the time integral part in the numerator of H_∞ performance index in (53) and the quadratic Lyapunov function in (71), we can get

$$\begin{aligned}&\textstyle\int_0^{t_f}[\tilde{e}_{j,i}^T(t)\tilde{Q}_{j,i}\tilde{e}_{j,i}(t) + u_{j,i}^T(t)R_{j,i}u_{j,i}(t)]dt \quad (73)\\ &= \textstyle\int_0^{t_f}[\tilde{e}_{j,i}^T(t)\tilde{Q}_{j,i}\tilde{e}_{j,i}(t) + u_{j,i}^T(t)R_{j,i}u_{j,i}(t) \\ &+\tfrac{dV_{e,j,i}(\tilde{e}_{j,i}(t))}{dt}]dt + V_{e,j,i}(\tilde{e}_{j,i}(0)) - V_{e,j,i}(\tilde{e}_{j,i}(t_f)) \\ &\le \textstyle\int_0^{t_f}\{\tilde{e}_{j,i}^T(t)\tilde{Q}_{j,i}\tilde{e}_{j,i}(t) + [\sum_{k=1}^{L_{j,i}} h_{k,j,i}(\tilde{e}_{j,i}(t))\tilde{K}_{k,j,i} \\ &\times\tilde{e}_{j,i}(t)]^T R_{j,i}[\textstyle\sum_{k=1}^{L_{j,i}} h_{k,j,i}(\tilde{e}_{j,i}(t))\tilde{K}_{k,j,i}\tilde{e}_{j,i}(t)] \\ &+\tilde{e}_{j,i}^T P_{j,i}[\textstyle\sum_{k=1}^{L_{j,i}} h_{k,j,i}(\tilde{e}_{j,i}(t))\{[\tilde{A}_{k,j,i} \\ &+\tilde{g}_{o,j,i}\tilde{K}_{k,j,i}]\tilde{e}_{j,i}(t) + \triangle\tilde{g}_{j,i}(\tilde{e}_{j,i}(t))\tilde{K}_{k,j,i}\tilde{e}_{j,i}(t) \\ &+\tilde{A}_{-k,j,i}\tilde{X}_{-j,i}(t) + \triangle\tilde{f}_{j,i}(\tilde{e}_{j,i}(t)) + \tilde{D}_{k,j,i}\tilde{v}_{j,i}(t)\}] \\ &+[\textstyle\sum_{k=1}^{L_{j,i}} h_{k,j,i}(\tilde{e}_{j,i}(t))\{[\tilde{A}_{k,j,i} + \tilde{g}_{o,j,i}\tilde{K}_{k,j,i}]\tilde{e}_{j,i}(t) \\ &+\triangle\tilde{g}_{j,i}(\tilde{e}_{j,i}(t))\tilde{K}_{k,j,i}\tilde{e}_{j,i}(t) + \tilde{A}_{-k,j,i}\tilde{X}_{-j,i}(t) \\ &+\triangle\tilde{f}_{j,i}(\tilde{e}_{j,i}(t)) + \tilde{D}_{k,j,i}\tilde{v}_{j,i}(t)\}]^T P_{j,i}\tilde{e}_{j,i}(t)\}dt \\ &+V_{e,j,i}(\tilde{e}_{j,i}(0))\end{aligned}$$

By Lemma 1 and *Assumption IV.1*, we obtain

$$\begin{aligned}&\tilde{e}_{j,i}^T P_{j,i}[\textstyle\sum_{k=1}^{L_{j,i}} h_{k,j,i}(\tilde{e}_{j,i}(t))\{[\tilde{A}_{k,j,i}+\tilde{g}_{o,j,i}\tilde{K}_{k,j,i}]\tilde{e}_{j,i}(t)\\&+\triangle\tilde{g}_{j,i}(\tilde{e}_{j,i}(t))\tilde{K}_{k,j,i}\tilde{e}_{j,i}(t)+\tilde{A}_{-k,j,i}\tilde{X}_{-j,i}(t)\\&+\triangle\tilde{f}_{j,i}(\tilde{e}_{j,i}(t))+\tilde{D}_{k,j,i}\tilde{v}_{j,i}(t)\}]\\&+[\textstyle\sum_{k=1}^{L_{j,i}} h_{k,j,i}(\tilde{e}_{j,i}(t))\{[\tilde{A}_{k,j,i}+\tilde{g}_{o,j,i}\tilde{K}_{k,j,i}]\tilde{e}_{j,i}(t)\\&+\triangle\tilde{g}_{j,i}(\tilde{e}_{j,i}(t))\tilde{K}_{k,j,i}\tilde{e}_{j,i}(t)+\tilde{A}_{-k,j,i}\tilde{X}_{-j,i}(t)\\&+\triangle\tilde{f}_{j,i}(\tilde{e}_{j,i}(t))+\tilde{D}_{k,j,i}\tilde{v}_{j,i}(t)\}]^T P_{j,i}\tilde{e}_{j,i}(t)\}dt\\&+V_{e,j,i}(\tilde{e}_{j,i}(0))\end{aligned} \tag{74}$$

$$\begin{aligned}&\leq \textstyle\sum_{k=1}^{L_{j,i}} h_{k,j,i}(\tilde{e}_{j,i}(t))\int_0^{t_f}\{\tilde{e}_{j,i}^T(t)[(\triangle\varepsilon_{j,i})^2\,\tilde{K}_{k,j,i}^T\tilde{K}_{k,j,i}\\&+P_{j,i}\tilde{A}_{k,j,i}+\tilde{A}_{k,j,i}^T P_{j,i}+P_{j,i}\tilde{g}_{o,j,i}\tilde{K}_{k,j,i}\\&+\tilde{K}_{k,j,i}^T\tilde{g}_{o,j,i}^T P_{j,i}+2P_{j,i}P_{j,i}+\tfrac{1}{\rho_{j,i}^2}P_{j,i}\tilde{D}_{k,j,i}\tilde{D}_{k,j,i}^T P_{j,i}\\&+\tfrac{1}{\rho_{j,i}^2}P_{j,i}\tilde{A}_{-k,j,i}\tilde{A}_{-k,j,i}^T P_{j,i}+\triangle F_{j,i}^T\triangle F_{j,i}]\tilde{e}_{j,i}(t)\\&+\rho_{j,i}^2\tilde{v}_{j,i}^T(t)\tilde{v}_{j,i}(t)+\rho_{j,i}^2\tilde{X}_{-j,i}^T(t)\tilde{X}_{-j,i}(t)\}dt\\&+V_{e,j,i}(\tilde{e}_{j,i}(0))\end{aligned}$$

Accordingly, from (73) and (74), we get

$$\begin{aligned}&\int_0^{t_f}[\tilde{e}_{j,i}^T(t)\tilde{Q}_{j,i}\tilde{e}_{j,i}(t)+u_{j,i}^T(t)R_{j,i}u_{j,i}(t)]dt\\&\leq \textstyle\sum_{k=1}^{L_{j,i}} h_{k,j,i}(\tilde{e}_{j,i}(t))\int_0^{t_f}\{\tilde{e}_{j,i}^T(t)[\tilde{Q}_{j,i}+\tilde{K}_{k,j,i}^T[R_{j,i}\\&+(\triangle\varepsilon_{j,i})^2 I]\tilde{K}_{k,j,i}+P_{j,i}\tilde{A}_{k,j,i}+\tilde{A}_{k,j,i}^T P_{j,i}\\&+P_{j,i}\tilde{g}_{o,j,i}\tilde{K}_{k,j,i}+\tilde{K}_{k,j,i}^T\tilde{g}_{o,j,i}^T P_{j,i}+2P_{j,i}P_{j,i}\\&+\tfrac{1}{\rho_{j,i}^2}P_{j,i}\tilde{A}_{-k,j,i}\tilde{A}_{-k,j,i}^T P_{j,i}+\triangle F_{j,i}^T\triangle F_{j,i}\\&+\tfrac{1}{\rho_{j,i}^2}P_{j,i}\tilde{D}_{k,j,i}\tilde{D}_{k,j,i}^T P_{j,i}]\tilde{e}_{j,i}(t)+\rho_{j,i}^2\tilde{v}_{j,i}^T(t)\tilde{v}_{j,i}(t)\\&+\rho_{j,i}^2\tilde{X}_{-j,i}^T(t)\tilde{X}_{-j,i}(t)\}dt+V_{e,j,i}(\tilde{e}_{j,i}(0))\end{aligned}$$

If Riccati-like inequality in (72) is satisfied, then the following inequality holds:

$$\begin{aligned}&\int_0^{t_f}[\tilde{e}_{j,i}^T(t)\tilde{Q}_{j,i}\tilde{e}_{j,i}(t)+u_{j,i}^T(t)R_{j,i}u_{j,i}(t)]dt\\&\leq V_{e,j,i}(\tilde{e}_{j,i}(0))+\rho_{j,i}^2\int_0^{t_f}[\tilde{v}_{j,i}^T(t)\tilde{v}_{j,i}(t)\\&+\tilde{X}_{-j,i}^T(t)\tilde{X}_{-j,i}(t)]dt\end{aligned} \tag{75}$$

which implies that

$$\frac{\begin{aligned}&\int_0^{t_f}[\tilde{e}_{j,i}^T(t)\tilde{Q}_{j,i}\tilde{e}_{j,i}(t)\\&+u_{j,i}^T(t)R_{j,i}u_{j,i}(t)]dt\\&-V_{e,j,i}(\tilde{e}_{j,i}(0))\end{aligned}}{\begin{aligned}&\int_0^{t_f}[\tilde{v}_{j,i}^T(t)\tilde{v}_{j,i}(t)\\&+\tilde{X}_{-j,i}^T(t)\tilde{X}_{-j,i}(t)]dt\end{aligned}}\leq \rho_{j,i}^2,\ \text{for } i\in\mathbb{N}_T, j\in\mathbb{N}_i$$

Therefore, if the Riccati-like inequalities in (72) are solved, the robust H_∞ decentralized collaborative team formation tracking control strategy for the jth leader-follower team formation subsystem in the ith hybrid team in (53) is guaranteed with a prescribed disturbance attenuation level $\rho_{j,i}^2$. On the other hand, if the external disturbances and the wireless communication couplings of the jth leader-follower team formation subsystem in the ith hybrid team are vanished, that is, $\tilde{v}_{j,i}(t)=0$ and $\tilde{X}_{-j,i}(t)=0$, the inequalities in (75) can be written in the bounded H_2 collaborative team formation tracking control design problem in (54).

From (54), the total energy of the jth leader-follower team formation subsystem in the ith hybrid team on the time interval $[0,\infty]$ is bounded by $V_{e,j,i}(\tilde{e}_{j,i}(0))$. As a result, as $t_f\to\infty$, team formation tracking error $\tilde{e}_{j,i}(t)$ will H_2 asymptotically converge to zero. The proof is completed. ■

By utilizing the collaborative team formation tracking control design in Theorem 2, the HJIs in (57) for the jth leader-follower team formation subsystem in the ith hybrid team can be transformed into the Riccati-like inequalities in (72). Nevertheless, due to the bilinear terms in (72), it is still too difficult and complex to solve the Riccati-like inequalities directly. Therefore, the following theorem is proposed to transform the Riccati-like inequalities into LMIs, which can be solved efficiently by MATLAB LMI TOOLBOX:

Theorem 3: If there exists common solution $W_{j,i}=W_{j,i}^T\in\mathbb{R}^{n_{e,j,i}\times n_{e,j,i}}>0$ and $Y_{k,j,i}\in\mathbb{R}^{n_{u,j,i}\times n_{e,j,i}}$ such that the following LMIs hold:

$$\begin{bmatrix}\Phi_{k,j,i} & * & * & *\\ Y_{k,j,i} & -\tilde{R}_{j,i}^{-1} & * & *\\ \tilde{Q}_{j,i}^{\frac{1}{2}}W_{j,i} & 0 & -I & *\\ \triangle F_{j,i}W_{j,i} & 0 & 0 & -I\end{bmatrix}<0 \tag{76}$$
$$\text{, for } i\in\mathbb{N}_T, j\in\mathbb{N}_i, k\in\{1,\cdots,L_{j,i}\}$$

with

$$\begin{aligned}\Phi_{k,j,i}&=\tilde{A}_{k,j,i}W_{j,i}+W_{j,i}\tilde{A}_{k,j,i}^T+\tilde{g}_{o,j,i}Y_{k,j,i}\\&\quad+Y_{k,j,i}^T\tilde{g}_{o,j,i}^T+2I+\tfrac{1}{\rho_{j,i}^2}\tilde{A}_{-k,j,i}\tilde{A}_{-k,j,i}^T\\&\quad+\tfrac{1}{\rho_{j,i}^2}\tilde{D}_{k,j,i}\tilde{D}_{k,j,i}^T\\ \tilde{R}_{j,i}&=R_{j,i}+(\triangle\varepsilon_i)^2 I\end{aligned}$$

then the robust H_∞ decentralized collaborative team formation tracking control law in (69) can be obtained from $\tilde{K}_{k,j,i}=Y_{k,j,i}W_{j,i}^{-1}$ and the robust H_∞ decentralized collaborative team formation tracking performance in (53) can be achieved with a prescribed disturbance attenuation level $\rho_{j,i}^2$.

Proof. Let $W_{j,i}=P_{j,i}^{-1}$ and $Y_{k,j,i}=\tilde{K}_{k,j,i}W_{j,i}$, for $i\in\mathbb{N}_T, j\in\mathbb{N}_i, k\in\{1,\cdots,L_{j,i}\}$. To begin with, by multiplying $W_{j,i}$ into both side of Riccati-like inequalities in (72), the Riccati-like inequalities can be reformulated as follows:

$$\begin{aligned}&W_{j,i}\tilde{Q}_{j,i}W_{j,i}+Y_{k,j,i}^T[R_{j,i}+(\triangle\varepsilon_{j,i})^2 I]Y_{k,j,i}+\tilde{A}_{k,j,i}W_{j,i}\\&+W_{j,i}\tilde{A}_{k,j,i}^T+\tilde{g}_{o,j,i}Y_{k,j,i}+Y_{k,j,i}^T\tilde{g}_{o,j,i}^T+2I\\&+\tfrac{1}{\rho_{j,i}^2}\tilde{A}_{-k,j,i}\tilde{A}_{-k,j,i}^T+W_{j,i}\triangle F_{j,i}^T\triangle F_{j,i}W_{j,i}\\&+\tfrac{1}{\rho_{j,i}^2}\tilde{D}_{k,j,i}\tilde{D}_{k,j,i}^T<0\end{aligned} \tag{77}$$

By Schur complement [45], the Riccati-like inequalities in (77) can be transformed as the following LMIs:

$$\begin{bmatrix}\Phi_{k,j,i} & * & * & *\\ Y_{k,j,i} & -\tilde{R}_{j,i}^{-1} & * & *\\ \tilde{Q}_{j,i}^{\frac{1}{2}}W_{j,i} & 0 & -I & *\\ \triangle F_{j,i}W_{j,i} & 0 & 0 & -I\end{bmatrix}<0$$
$$\text{, for } i\in\mathbb{N}_T, j\in\mathbb{N}_i, k\in\{1,\cdots,L_{j,i}\}$$

where $\Phi_{k,j,i}=\tilde{A}_{k,j,i}W_{j,i}+W_{j,i}\tilde{A}_{k,j,i}^T+\tilde{g}_{o,j,i}Y_{k,j,i}+Y_{k,j,i}^T\tilde{g}_{o,j,i}^T+2I+\frac{1}{\rho_{j,i}^2}\tilde{A}_{-k,j,i}\tilde{A}_{-k,j,i}^T+\frac{1}{\rho_{j,i}^2}\tilde{D}_{k,j,i}\tilde{D}_{k,j,i}^T$;

$\tilde{R}_{j,i} = R_{j,i} + (\triangle\varepsilon_{j,i})^2 I$; $\tilde{Q}_{j,i}^{\frac{1}{2}}$ are the Cholesky decomposition of weighting matrix $\tilde{Q}_{j,i}$,for $i \in \mathbb{N}_T, j \in \mathbb{N}_i$. As a result, the Riccati-like inequalities-constrained problem in (72) is transformed into the equivalent LMIs in (76). The proof is completed. ■

Remark 5: Without considering the external disturbances and communication coupling in (70), if there exists common solution $W_{j,i} = W_{j,i}^T \in \mathbb{R}^{n_{e,j,i}\times n_{e,j,i}} > 0$ and $Y_{k,j,i} \in \mathbb{R}^{n_{u,j,i}\times n_{e,j,i}}$ such that the following LMIs hold:

$$\begin{bmatrix} \Phi_{k,j,i} & * & * & * \\ Y_{k,j,i} & -\tilde{R}_{j,i}^{-1} & * & * \\ \tilde{Q}_{j,i}^{\frac{1}{2}} W_{j,i} & 0 & -I & * \\ \triangle F_{j,i} W_{j,i} & 0 & 0 & -I \end{bmatrix} < 0 \quad (78)$$
$$, \text{for } i \in \mathbb{N}_T, j \in \mathbb{N}_i, k \in \{1, \cdots, L_{j,i}\}$$

with

$$\Phi_{k,j,i} = \tilde{A}_{k,j,i} W_{j,i} + W_{j,i}\tilde{A}_{k,j,i}^T + \tilde{g}_{o,j,i} Y_{k,j,i} + Y_{k,j,i}^T \tilde{g}_{o,j,i}^T + 2I$$
$$\tilde{R}_{j,i} = R_{j,i} + (\triangle\varepsilon_i)^2 I$$

then the H_2 decentralized collaborative team formation tracking control law in (69) can be obtained from $\tilde{K}_{k,j,i} = Y_{k,j,i} W_{j,i}^{-1}$ and the H_2 decentralized collaborative team formation tracking performance in (54) can be achieved by minimize the upperbound $V_{e,j,i}(\tilde{e}_{j,i}(0)) = \tilde{e}_{j,i}^T(0) W_{j,i}^{-1} \tilde{e}_{j,i}(0)$. Therefore, if we want to achieve the optimal H_2 decentralized collaborative team formation tracking control, we need to solve the following problem [50], [51]:

$$\min_{W_{j,i}>0, Y_{k,j,i}} \tilde{e}_{j,i}^T(0) W_{j,i}^{-1} \tilde{e}_{j,i}(0) \quad (79)$$
$$\text{subject to LMI in (78)}$$

which is equivalent to the following constrained optimization:

$$\min_{W_{j,i}>0, Y_{k,j,i}} \lambda_{j,i} \quad (80)$$
$$\text{subject to} \begin{bmatrix} \lambda_{j,i} I & \tilde{e}_{j,i}^T(0) \\ \tilde{e}_{j,i}(0) & -W_{j,i} \end{bmatrix} < 0 \text{ and (78)}$$

Based on Theorem 3, the design procedure of robust H_∞ decentralized collaborative team formation tracking controller for the jth leader-follower team formation subsystem in the ith hybrid team can be described as follows:

1) Construct the tractor-trailer dynamic system (25) and biped robot dynamic system (26) with consideration of the external disturbances and wireless communication coupling terms.
2) Specify the smooth desired trajectories of collaborative team formation by adequate reference models in (27) and (28) with some desired transient response (i.e., $A_{r,0,i}$, $B_{r,0,i}$ for leaders and $A_{r,j,i}$, $B_{r,j,i}$ for followers) and some desired time-varying team formation offsets ($d_{0,i}(t)$ for leaders in (29) with a desired formation shape $[d_{0,1}^T(t), d_{0,2}^T(t), \cdots, d_{0,N_T}^T(t)]^T$ and $d_{j,i}(t)$ for followers in (30) with a desired formation shape $[d_{1,i}^T(t), d_{2,i}^T(t), \cdots, d_{N_i,i}^T(t)]^T$), and select the augmented weighting matrices (i.e., $\tilde{Q}_{j,i}$ and $R_{j,i}$) and the prescribed external disturbance attenuation level $\rho_{j,i}^2$ of the robust H_∞ decentralized collaborative team formation tracking control strategy in (41) and (42).
3) Augment the collaborative team formation error dynamic system with leader-follower structure in (45) to simplify the design procedure of robust H_∞ decentralized collaborative team formation tracking control strategy in (53).
4) Utilize the tensor product model transformation and the numerical LPV modeling method to approximate the augmented collaborative leader-follower team formation dynamic system in (70) and solve LMIs in (76) for $W_{j,i}$ and $Y_{k,j,i}$ by MATLAB LMI TOOLBOX to get controller gains $\tilde{K}_{k,j,i} = Y_{k,j,i} W_{j,i}^{-1}$ in (69) for each LPV model.
5) Employ the parallel distributed compensation (PDC) method to get decentralized collaborative team formation tracking control strategy in (69).

VI. SIMULATION RESULTS

In this section, to demonstrate the effectiveness of the proposed robust H_∞ decentralized collaborative team formation tracking control strategy, a simulation example of a collaborative team formation tracking task for the hybrid teams of wheeled vehicles (i.e., leader) and biped robots (i.e., followers) is provided. In this simulation, there are three hybrid teams to be asked to track desired trajectories to achieve an ideal collaborative team formation shape as shown in Fig. 5, and each hybrid team consists of one tractor-trailer (i.e, leader) and six biped robots (i.e., follower). In addition, with the help of robust H_∞ decentralized collaborative team formation tracking control strategy, not only the number of hybrid teams but also the number of agents in each hybrid team can be easily extended to a very large scale with some adequate arrangements.

A. PARAMETER SETTING

Symbol	Value	Symbol	Value
l_0	0.03 m	m_{t1}	0.35 kg
l_1	0 m	$m_{wL} = m_{wR}$	0.03 kg
d	0.2 m	$I_{\phi 0}$	0.005116 kg·m^2
w	0.06 m	$I_{\phi 1}$	0.043416 kg·m^2
m_{t0}	1 kg	r	0.025 m

TABLE 1: Tractor-trailer kinematic and dynamic parameters [38]

For a tractor-trailer as the leader in a hybrid team formation, the coordinate configuration is shown in Fig. 1, and the corresponding kinematic and dynamic parameters are listed in TABLE 1. In addition, for a biped robot as a follower in a hybrid team formation, the coordinate configuration and corresponding dynamic parameters are shown in Fig. 2 and TABLE 2, respectively. Afterwards, for the reference models in (27) and (28) of leaders and followers, respectively, in

Symbol	Value (kg·m^2)
I_0	10^{-2}Pos$(3.603, 2.21, 3.82, 0, 0, 0)$
$I_1 = I_2$	10^{-4}Pos$(2, 10, 9, 0, 0, 0)$
$I_3 = I_4$	10^{-4}Pos$(6, 17, 17, 0, 0, 0)$
I_5	10^{-4}Pos$(433, 404, 56, 3, 29, -20)$
I_6	10^{-4}Pos$(433, 404, 56, -3, 29, 20)$
I_7	10^{-4}Pos$(197, 196, 57, 3, -29, -14)$
I_8	10^{-4}Pos$(197, 196, 57, -3, 29, 14)$
$I_9 = I_{10}$	10^{-4}Pos$(6, 17, 17, 0, 0, 0)$
$I_{11} = I_{12}$	10^{-5}Pos$(22, 99, 91, 0, -0.1, 0)$

with $\text{Pos}(I_{xx},I_{yy},I_{zz},I_{xy},I_{xz},I_{yz}) = \begin{bmatrix} I_{xx} & I_{xy} & I_{xz} \\ I_{xy} & I_{yy} & I_{yz} \\ I_{xz} & I_{yz} & I_{zz} \end{bmatrix}$

(a) The biped-robot link inertia I_i, for $i \in \{0, 1, ..., 12\}$, which denote the inertia matrix of the ith center-of-mass reference frame.

Symbol	Value (kg·m^2)
COM_1	Trans$(-0.017, +0.035, -0.1157)$
COM_2	Trans$(-0.017, -0.035, -0.1157)$
COM_3	Trans$(-0.073, +0.035, -0.1192)$
COM_4	Trans$(-0.073, -0.035, -0.1192)$
COM_5	Trans$(+0.017, +0.028, -0.3392)$
COM_6	Trans$(+0.017, -0.028, -0.3392)$
COM_7	Trans$(-0.007, +0.035, -0.3972)$
COM_8	Trans$(-0.007, -0.031, -0.3972)$
COM_9	Trans$(-0.016, +0.037, -0.4177)$
COM_{10}	Trans$(-0.016, -0.037, -0.4177)$
COM_{11}	Trans$(-0.075, +0.035, -0.5222)$
COM_{12}	Trans$(-0.075, -0.035, -0.5222)$

with $\text{Trans}(x, y, z) = \begin{bmatrix} I_3 & [x, y, z]^T \\ 0_{1\times 3} & I \end{bmatrix}$

(b) The biped-robot center-of-mass reference frame COM_i, for $i \in \{0, 1, ..., 12\}$ with respect to the local body frame $COM_0 = I_4$

Symbol	Value (m)
L_1	0.035
L_2	0.0907
L_3	0.0285
$L_4 = L_5$	0.11
L_6	0.0305

(c) The biped-robot link length L_i, for $i \in \{1, ..., 6\}$.

Symbol	Value (kg)
m_0	6.869
$m_1 = m_2$	0.243
$m_3 = m_4$	1.405
$m_5 = m_6$	3.095
$m_7 = m_8$	2.401
$m_9 = m_{10}$	1.045
$m_{11} = m_{12}$	0.233

(d) The biped-robot link mass m_i, for $i \in \{0, 1, ..., 12\}$.

TABLE 2: Generic biped-robot kinematic and dynamic parameters [48]

the collaborative team formation system, the system matrices are set by $A_{r,0,i} = A_{r,j,i} = -10I$ and $B_{r,0,i} = B_{r,j,i} = 10I$ such that $X_{r,0,i}(t)$ approaches to $r_{0,i}(t)$ and $X_{r,j,i}(t)$ approaches to $r_{j,i}(t)$ at the steady state with a convergence rate e^{-10t}. Moreover, for the ideal trajectory of leader in (29), the reference input in (27) of the leader in the team 1 is firstly set as $r_{0,1}(t)$, which is shown in the line in Fig. 5, and the leaders in the team 2 and team 3 are set as $r_{0,2}(t) = r_{0,1}(t) + d_{0,2}(t)$ and $r_{0,3}(t) = r_{0,1}(t) + d_{0,3}(t)$ with adequate time-varying offsets $d_{0,2}(t)$ and $d_{0,3}(t)$, respectively. Furthermore, from (28) and (30), the formation offsets of followers are prescribed based on the trajectories of leaders in the same hybrid team, for instance, the ideal trajectory of the 2th follower in the hybrid team 2 is designed by $r_{2,2}(t) = r_{0,2}(t) + d_{2,2}(t)$, where $r_{0,2}(t)$ is the ideal trajectory of leader in the hybrid team 2 and $d_{2,2}(t)$ is the adequate time-varying offset for the 2th follower in the hybrid team 2. In this simulation, the external disturbances are set as Gaussian noises with zero means and 0.1 variances. Moreover, since communication requirements between agents in each team, several interconnected coupling effects will emerge such as co-channel interference in communication, which makes the agents in the same team being interfered by each other. Therefore, the wireless communication coupling terms $\{f_{0,j,i}(X_{0,i}(t))\}_{j=1,j\neq i}^{N_T}$ and $\{f_{j,k,i}(X_{j,i}(t))\}_{k=1,k\neq j}^{N_i}$ in (25) and (26) are given as follows:

$$\begin{aligned} f_{0,j,i}(X_{0,i}(t)) &= 0.01diag(x_{0,i,1}(t), \cdots, x_{0,i,n_L}(t)) \\ &, \text{for } i \in \{1, 2, 3\} \\ f_{j,k,i}(X_{j,i}(t)) &= 0.01diag(x_{j,i,1}(t), \cdots, x_{j,i,n_F}(t)) \\ &, \text{for } i \in \{1, 2, 3\},\ j \in \{1, \cdots, 6\} \end{aligned}$$

where $x_{0,i,n}(t)$ is the nth component in $X_{0,i}(t)$ (i.e., the state of leader in the ith hybrid team) and $x_{j,i,n}(t)$ is the nth component in $X_{j,i}(t)$ (i.e., the state of the jth follower in the ith hybrid team).

Based on the above parameter setting, we employ the tensor product model transformation and numerical LPV modeling method in Section V to approximate the biped robot and tractor-trailer. Consequently, the augmented collaborative team formation tracking error dynamic system for each leader-follower hybrid team formation subsystem in (70) can be constructed as follows:

$$\begin{aligned} \dot{\tilde{e}}_{j,i}(t) = \sum_{k=1}^{160} & h_{k,j,i}(\tilde{e}_{j,i}(t))\{[\tilde{A}_{k,j,i}\tilde{e}_{j,i}(t) + \triangle\tilde{f}_{j,i}(\tilde{e}_{j,i}(t))] \\ & + [\tilde{g}_{o,j,i} + \triangle\tilde{g}_{j,i}(\tilde{e}_{j,i}(t))]\, u_{j,i}(t) + \tilde{D}_{k,j,i}\tilde{v}_{j,i}(t) \\ & + \tilde{A}_{-k,j,i}\tilde{X}_{-j,i}(t)\} \\ & , \text{for } i \in \{1, 2, 3\},\ j \in \{0, 1, 2..., 6\} \end{aligned}$$

where $\{\tilde{A}_{k,j,i}, \tilde{D}_{k,j,i}, \tilde{A}_{-k,j,i}\}$ are the system matrices obtained by tensor product model transformation with sampling region within $\tilde{X}_{e,i}(t) \in [-1, 1]^4$, $\tilde{\mathcal{V}}_{t,i}^T(t) \in [-1, 1]^2$, $\tilde{q}_{j,i}(t) \in [-\pi/2, \pi/2]^{12}$, $\tilde{X}_{R,j,i}(t) \in [-1, 1]^3$, $V_{h,j,i}(t) \in [-1, 1]^{12}$. Furthermore, by the proposed robust H_∞ decentralized collaborative team formation tracking control design strategy in (41) and (42), the relative weighting matrices and prescribed external disturbance attenuation level are designed as follows:

$$\begin{aligned} & Q_{1,0,i} = 5 \times 10^{-3} diag(I_2, 0.2I_2), Q_{2,0,i} = 10^{-3}I_2 \\ & , R_{0,i} = 10^{-3}I_2, \bar{Q}_{1,j,i} = 10^{-5}I_4, Q_{2,j,i} = 10^{-6}I_3 \\ & , R_{j,i} = 10^{-4}I_{12}, \rho_{j,i} = 6.5 \\ & , \text{for } i \in \{1, 2, 3\},\ j \in \{0, 1, 2..., 6\} \end{aligned}$$

Since the augmented leader-follower hybrid system consists of the tractor-trailer dynamic system and the biped-robot dynamic system, apart from the unknown external

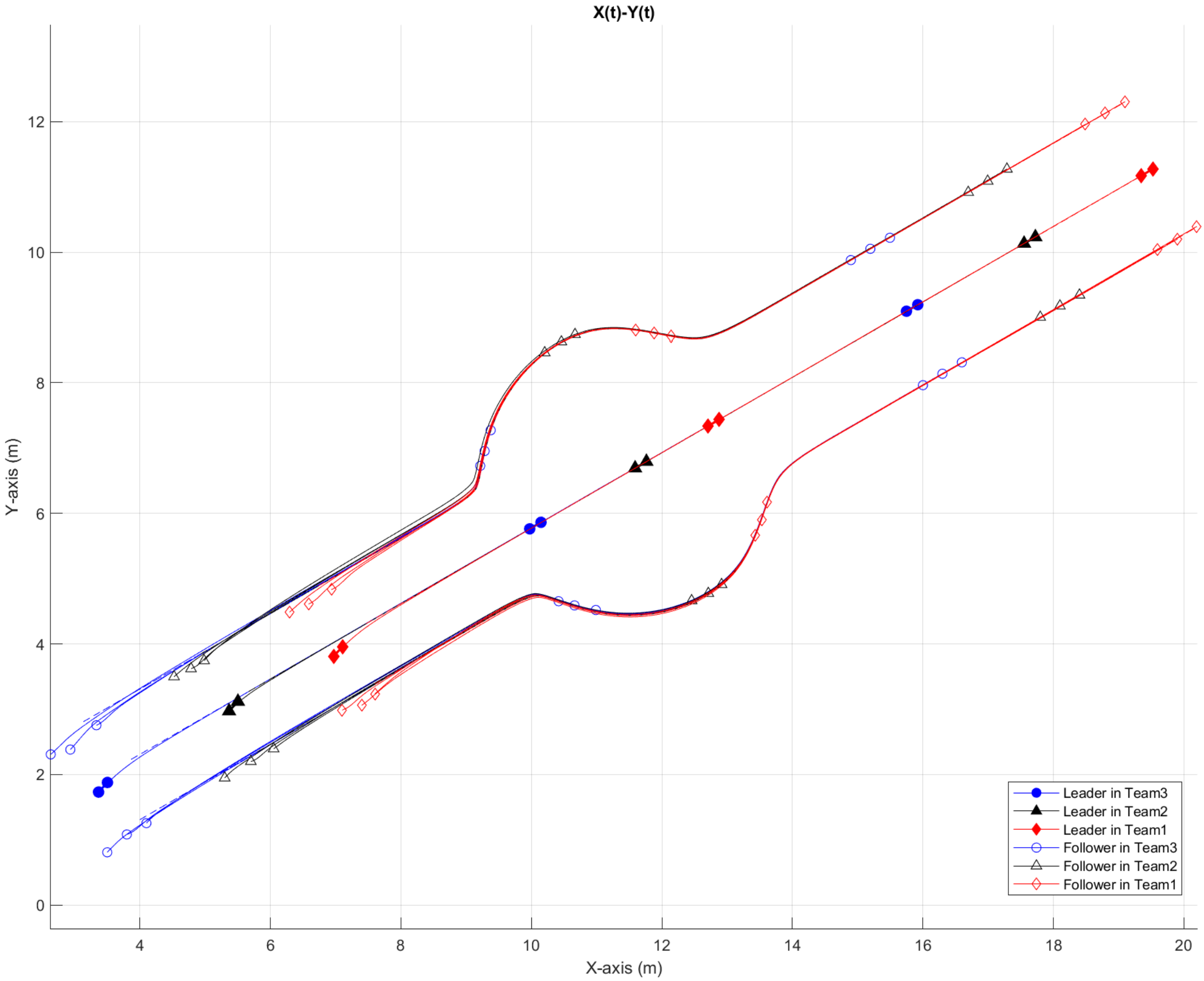

FIGURE 5: The planar trajectory of collaborative team formation of three teams with one tractor-trailer as a leader and six biped robots as followers in each team. The mark indexes represent the collaborative team formation tracking moment at 0s, 80s, and 170s, respectively. The solid mark index represents the position of tractor-trailer, while the hollow mark index represents the biped-robot position.

disturbances, the characteristic of different dynamic systems and the corresponding couplings must be considered. Therefore, to deal with the worst-case external disturbances and the worst-case couplings, the robust H_∞ decentralized team formation tracking control strategy is designed for 3 hybrid teams conservatively. In this simulation, due to performing many inequalities to obtain Riccati-like inequalities in (72) in the proof process of Theorem 2 and the conservative solutions of LMIs in (76), the prescribed external disturbance attenuation level $\rho_{j,i}$ is set as 6.5. After all, the LMIs for the robust H_∞ decentralized collaborative team formation tracking control design problem in (76) can be easily solved by MATLAB LMI TOOLBOX to obtain the controller gain in each LPV model and the decentralized collaborative team formation tracking control strategy in (69) can be synthesized via PDC method.

B. RESULTS AND DISCUSSIONS

The simulation results are shown in Figs. 5-13. In Fig. 5, the planar representation of collaborative team formation trajectory shows that each hybrid team can track their desired trajectory via the proposed robust H_∞ decentralized collaborative team formation tracking control strategy. Additionally, the followers can also plan their trajectories beforehand to avoid the obstacles on their original routes. In Fig. 6, the team formation trajectory of each leader could track its own desired trajectory under the influence of external disturbance and wireless communication couplings. In Fig. 7, it can be noticed that the steady-state fluctuations of velocity error are more obvious than the position error in Fig. 6. There are two

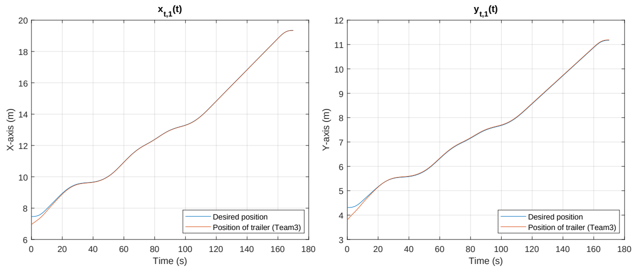

(a) The team formation tracking trajectory of trailer on x-axis (b) The team formation tracking trajectory of trailer on y-axis

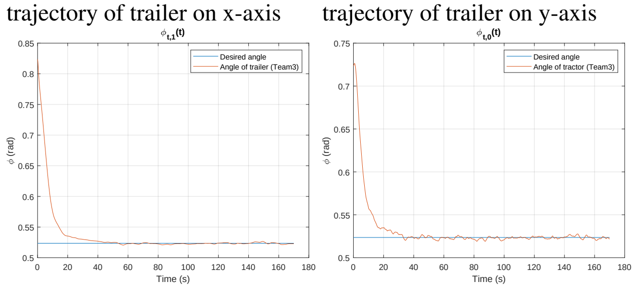

(c) The orientation tracking trajectory of trailer along z-axis (d) The orientation tracking trajectory of tractor along z-axis

FIGURE 6: The team formation tracking trajectory of the orientation of tractor-trailer (i.e., leader) in team 3

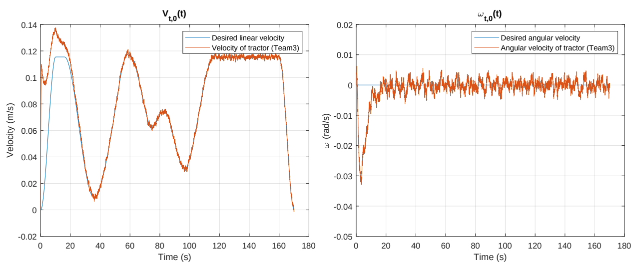

(a) The linear velocity tracking trajectory of leader (b) The angular velocity tracking trajectory of leader

FIGURE 7: The velocity tracking trajectory of tractor-trailer (i.e., leader) in team 3

reasons: One is that the weighting matrix $Q_{2,0,i} = 10^{-3} < Q_{1,0,i} = 5 \times 10^{-3}$, for $i \in \{1, 2, 3\}$. With more light penalty on velocity tracking error will lead to a larger fluctuations. The other one is that the external disturbances influence on the system state from the velocity terms directly. On the other hand, it can be also noticed that the steady-state fluctuations of velocity error are around 0.005, which demonstrates the robustness of the collaborative team formation system under the proposed robust H_∞ decentralized collaborative team formation tracking control strategy. In Fig. 8, the biped-robot team formation tracking trajectory presents that the followers in each hybrid team can also track their desired trajectories to achieve their desired team formation. In the meanwhile, in Fig. 9, the redundant joints of biped robot can be controlled to keep an upright torso while walking under the effect of external disturbance and interactive communication couplings. Subsequently, the control inputs of the tractor-

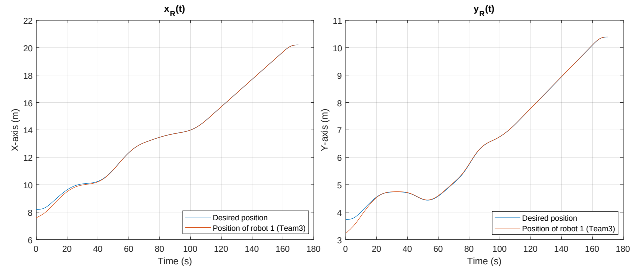

(a) The team formation tracking trajectory of biped robot 1 on x-axis (b) The team formation tracking trajectory of biped robot 1 on y-axis

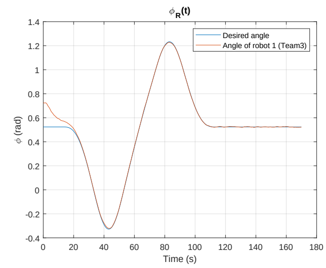

(c) The orientation tracking trajectory of biped robot 1 along z-axis

FIGURE 8: The team formation tracking trajectory of biped robot 1 (i.e., follower 1) in team 3

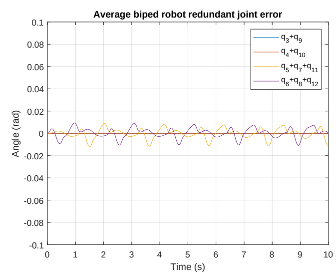

FIGURE 9: The average joint-space position tracking error of biped robots. For the convenience of illustration, only the results in the first 10 seconds are presented.

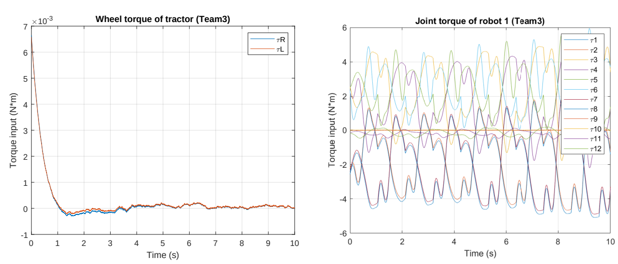

(a) The wheel torque of tractor-trailer in team 3 (b) The joint torque of biped robot 1 in team 3

FIGURE 10: The input torque of tractor-trailer and biped robot 1 in team 3. For the convenience of illustration, only the results in the first 10 seconds are presented.

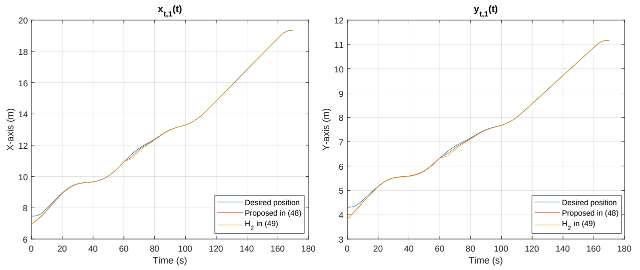

(a) The team formation tracking trajectory of trailer on x-axis (b) The team formation tracking trajectory of trailer on y-axis

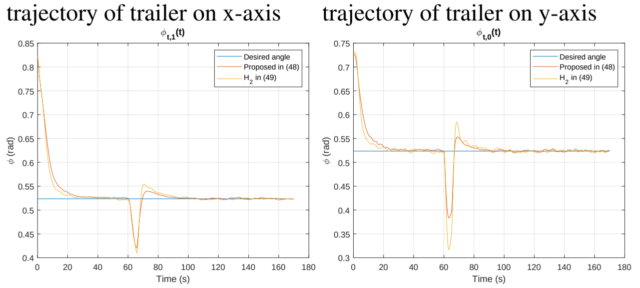

(c) The orientation tracking trajectory of trailer along z-axis (d) The orientation tracking trajectory of tractor along z-axis

FIGURE 11: The team formation tracking trajectory of tractor-trailer (i.e., leader) in team 3 by the proposed robust H_∞ tracking scheme and the optimal H_2 tracking scheme.

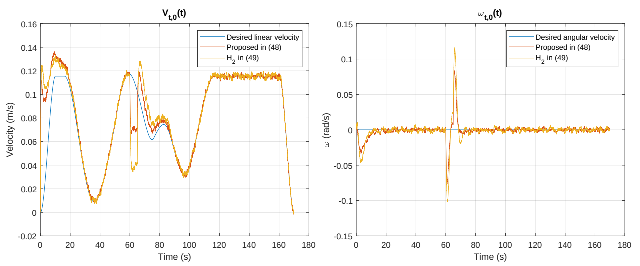

(a) The linear velocity tracking trajectory of leader (b) The angular velocity tracking trajectory of leader

FIGURE 12: The velocity tracking trajectory of tractor-trailer (i.e., leader) in team 3 by the proposed robust H_∞ tracking scheme and the optimal H_2 tracking scheme.

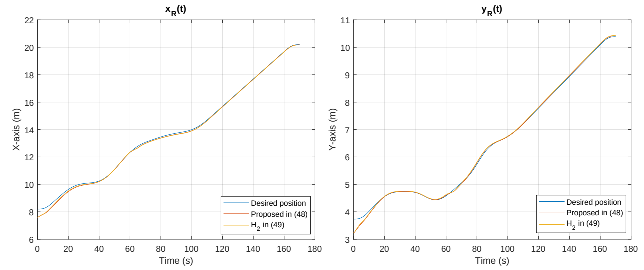

(a) The team formation tracking trajectory of biped robot 1 on x-axis (b) The team formation tracking trajectory of biped robot 1 on y-axis

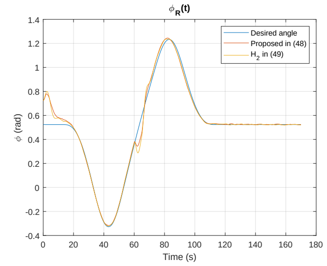

(c) The orientation tracking trajectory of biped robot 1 along z-axis

FIGURE 13: The team formation tracking trajectory of biped robot 1 (i.e., follower 1) in team 3 by the proposed robust H_∞ tracking scheme and the optimal H_2 tracking scheme.

trailer and biped robot are displayed in Fig. 10, which are calculated by Recursive Newton-Euler Algorithm with computation complexity $O(n)$ such that the proposed robust H_∞ decentralized collaborative team formation tracking control strategy is applicable for practical implementation. In Figs. 6-9, the transient responses of the leader-follower hybrid team formation subsystem are around 0s-40s which are mainly caused by the effect of initial conditions. By the proposed robust H_∞ decentralized tracking control strategy in (53), the effect of the initial condition can be efficiently attenuated without a serious overshoot. Since the effect of unavailable external disturbances, reference inputs and couplings $\Theta_{j,i}$ in (53) on the leader-follower hybrid team formation subsystem is efficiently attenuated by the proposed robust H_∞ decentralized collaborative team formation tracking control strategy in (53), the steady-state collaborative team formation tracking error of the leader-follower team formation subsystem becomes small. In addition, the transient response time in Figs. 6-8 is around 0s-40s, which is relative short for the overall collaborative team formation tracking control time $t_f = 170$s. As a result, after calculating the robust H_∞ decentralized collaborative team formation tracking control index in (53), the real average attenuation level of the leader-follower team formation subsystem $\bar{\rho} = 7.03 \times 10^{-7}$ is very small relative to the designed attenuation level $\rho_{j,i} = 6.5$, for $i \in \{1,2,3\}$, $j \in \{0,1,2...,6\}$. Finally, the optimal H_2 decentralized tracking control strategy in (64) or (80) is carried out and compared with the proposed robust H_∞ decentralized collaborative team formation tracking control strategy in (53). The compared results are shown in Figs. 11-13. To illustrate the difference of the robustness between two methods, the external disturbances of the unit steps with magnitude -0.2 are also added around 60s-65s to perform the suddenly loading change on the tractor-trailers and biped robots during the collaborative team formation reference tracking process. In the optimal H_2 decentralized collaborative team formation tracking control design procedure, the effect of external disturbance has not been considered. Therefore, in Figs. 11-13, when the suddenly loading change occurs around 60s-65s, the transient responses of the system states via optimal H_2 decentralized collaborative team formation tracking control strategy are more dramatic than the ones by the proposed robust H_∞ decentralized collaborative team formation tracking control strategy, especially in Fig. 12.

VII. CONCLUSION

In this study, a robust H_∞ decentralized collaborative team formation tracking control strategy is proposed to deal with the collaborative team formation tracking problems of hybrid teams of tractor-trailers and biped robots under the influence of unknown external disturbances and wireless communication couplings. Moreover, by the proposed robust H_∞ decentralized collaborative team formation tracking control strategy, if the external disturbances and the wireless communication couplings vanish, the H_2 collaborative team formation tracking performance can be achieved too. To begin with, the dynamic model of tractor-trailer and hybrid joint/task-space dynamic model of biped robot are constructed. Afterwards, a general augmented collaborative leader-follower team formation structure is proposed to represent two different dynamic models and mimic the collaborative team formation architecture of the real-world tractor-trailer/biped-robot hybrid dynamic systems. Subsequently, the reference model technique is employed with adequate time-varying team formation offset as reference input to generate any desired smooth trajectories with a desired team formation shape for the collaborative time-varying team formation of leaders and followers. Therefore, the collaborative team formation control design problem becomes a model reference tracking control design problem to simplify the following control design procedure. Further, by the general augmented collaborative leader-follower hybrid team formation subsystem, the reference tracking control strategy for the desired collaborative team formation of tractor-trailer as the leader and the biped robots as followers in each hybrid team formation subsystem can be designed simultaneously. By the proposed robust H_∞ decentralized collaborative team formation tracking control strategy, the original collaborative team formation tracking problem can be transformed into a set of independent HJI-constrained problems. Nonetheless, there still does not exist an efficient method to cope with the complicate HJI-constrained problems. Therefore, the numerical LPV modeling method is proposed such that each HJI-constrained problem is converted into a set of LMI-constrained problems which can be efficiently solved by MATLAB LMI TOOLBOX. Since an agent (i.e., a leader or a follower) in the collaborative team formation tracking control can be designed and controlled independently by the proposed robust H_∞ decentralized collaborative team formation tracking control strategy, the number of hybrid team and the member in each hybrid team of the collaborative team formation of biped robots and wheeled vehicles can be extended to a very large scale. Finally, the simulation results are provided to illustrate the design procedure and validate the hybrid team formation tracking performance of the proposed robust H_∞ decentralized collaborative team formation tracking control strategy in comparison with the optimal H_2 collaborative team formation tracking control strategy. In the future researches, we will focus on the collaborative team formation tracking control of hybrid teams of UAVs, biped robots and tractor-trailers. By the collaboration among more types of autonomous mobile robots, more complex and dangerous tasks can be achieved more safely and efficiently.

REFERENCES

[1] M. A. K. Niloy *et al.*, "Critical design and control issues of indoor autonomous mobile robots: a review," *IEEE Access*, vol. 9, pp. 35338-35370, Feb. 2021.

[2] I. Park, J. Kim and J. Oh, "Online biped walking pattern generation for humanoid Robot KHR-3(KAIST Humanoid Robot - 3: HUBO)," in *Proc. 2006 6th IEEE-RAS Int. Conf. Humanoid Robot*, pp. 398-403.

[3] T. Sato, S. Sakaino and K. Ohnishi, "Real-time walking trajectory generation method with three-mass models at constant body height for three-dimensional biped robots," *IEEE Trans. Ind. Electron.*, vol. 58, no. 2, pp. 376-383, Feb. 2011.

[4] T. S. Li, Y. Su, S. Liu, J. Hu and C. Chen, "Dynamic balance control for biped robot walking using sensor fusion, kalman filter, and fuzzy logic," *IEEE Trans. Ind. Electron.*, vol. 59, no. 11, pp. 4394-4408, Nov. 2012.

[5] Q. Huang *et al.*, "Planning walking patterns for a biped robot," *IEEE Trans. Robot. Automat.*, vol. 17, no. 3, pp. 280-289, Jun. 2001.

[6] K. Erbatur and O. Kurt, "Natural ZMP trajectories for biped robot reference generation," *IEEE Trans. Ind. Electron.*, vol. 56, no. 3, pp. 835-845, Mar. 2009.

[7] S. Kajita *et al.*, "Biped walking pattern generation by using preview control of zero-moment point," in *Proc. 2003 IEEE Int. Conf. Robot. Autom.*, vol.2, pp. 1620-1626.

[8] E. R. Westervelt, J. W. Grizzle and D. E. Koditschek, "Hybrid zero dynamics of planar biped walkers," *IEEE Trans. Automat. Contr.*, vol. 48, no. 1, pp. 42-56, Jan. 2003.

[9] C. Chevallereau, J. W. Grizzle and C. Shih, "Asymptotically stable walking of a five-link underactuated 3-D bipedal robot," *IEEE Trans. Robot.*, vol. 25, no. 1, pp. 37-50, Feb. 2009.

[10] T. C. Lee, K. T. Song, C. H. Lee and C. C. Teng, "Tracking control of unicycle-modeled mobile robots using a saturation feedback controller," *IEEE Trans. Control Syst. Technol.*, vol. 9, no. 2, pp. 305-318, Mar. 2001.

[11] P. Coelho and U. Nunes, "Path-following control of mobile robots in presence of uncertainties," *IEEE Trans. Robot. Automat.*, vol. 21, no. 2, pp. 252-261, Apr. 2005.

[12] A. P. Aguiar and J. P. Hespanha, "Trajectory-tracking and Path-following of underactuated autonomous vehicles with parametric modeling uncertainty," *IEEE Trans. Automat. Contr.*, vol. 52, no. 8, pp. 1362-1379, Aug. 2007.

[13] B. S. Park, S. J. Yoo, J. B. Park and Y. H. Choi, "A simple adaptive control approach for trajectory tracking of electrically driven nonholonomic mobile robots," *IEEE Trans. Control Syst. Technol.*, vol. 18, no. 5, pp. 1199-1206, Sept. 2010.

[14] A. K. Khalaji and S. A. A. Moosavian, "Robust adaptive controller for a tractor–trailer mobile robot," *IEEE/ASME Trans. Mechatron.*, vol. 19, no. 3, pp. 943-953, Jun. 2014.

[15] E. Kayacan, H. Ramon and W. Saeys, "Robust trajectory tracking error model-based predictive control for unmanned ground vehicles," *IEEE/ASME Trans. Mechatron.*, vol. 21, no. 2, pp. 806-814, Apr. 2016.

[16] B. S. Chen, C. S. Wu and H. J. Uang, "A minimax tracking design for wheeled vehicles with trailer based on adaptive fuzzy elimination scheme," *IEEE Trans. Control Syst. Technol.*, vol. 8, no. 3, pp. 418-434, May 2000.

[17] Y. Zhang and H. Mehrjerdi, "A survey on multiple unmanned vehicles formation control and coordination: normal and fault situations," in *Proc. 2013 Int. Conf. Unmanned Airc. Syst. (ICUAS)*, pp. 1087-1096.

[18] E. Seraj and M. Gombolay, "Coordinated control of UAVs for human-centered active sensing of wildfires," in *Proc. 2020 American Control Conference (ACC)*, pp. 1645-1652.

[19] C. Luo, J. Nightingale, E. Asemota and C. Grecos, "A UAV-cloud system for disaster sensing applications," in *Proc. 2015 IEEE Veh. Technol. Conf. (VTC Spring)*, pp. 1-5.

[20] A. Mora, Javier, *et al.* "Multi-robot formation control and object transport in dynamic environments via constrained optimization." *Int. J. Rob. Res.*, vol. 36, no. 9, pp. 1000–1021, Aug. 2017.

[21] M. C. Gombolay, R. J. Wilcox and J. A. Shah, "Fast scheduling of robot teams performing tasks with temporospatial constraints," *IEEE Trans. Robot. Automat.*, vol. 34, no. 1, pp. 220-239, Feb. 2018.

[22] Y. Sabri, N. El Kamoun and F. Lakrami, "A survey: centralized, decentralized, and distributed control scheme in smart grid systems," in *Proc. 2019 7th Mediterranean Congress of Telecommunications (CMT)*, pp. 1-11.

[23] M. Y. Lee, B. S. Chen, C. Y. Tsai and C. L. Hwang, "Stochastic H_∞ Robust decentralized tracking control of large-scale team formation UAV network system with time-varying delay and packet dropout under interconnected couplings and wiener fluctuations," *IEEE Access*, vol. 9, pp. 41976-41997, 2021.

[24] C. S. Tseng and B. S. Chen, "H_∞ decentralized fuzzy model reference tracking control design for nonlinear interconnected systems," *IEEE Trans. Fuzzy Syst.*, vol. 9, no. 6, pp. 795-809, Dec. 2001.

[25] G. Liu and S. Zhang, "A survey on formation control of small satellites," *Proc. IEEE*, vol. 106, no. 3, pp. 440-457, Mar. 2018.

[26] J. R. T. Lawton, R. W. Beard and B. J. Young, "A decentralized approach to formation maneuvers," *IEEE Trans. Robot. Automat.*, vol. 19, no. 6, pp. 933-941, Dec. 2003.

[27] B. S. Chen, C. P. Wang and M. Y. Lee, "Stochastic robust team tracking control of multi-UAV networked system under wiener and poisson random fluctuations," *IEEE Trans. Cybern.*, pp. 1-14, Jan. 2020.

[28] P. Ogren, M. Egerstedt and X. Hu, "A control Lyapunov function approach to multi-agent coordination," in *Proc. IEEE Conf. Decis. Control*, pp. 1150-1155 vol.2, Dec. 2001.

[29] B. S. Chen, Y. Y. Tsai and M. Y. Lee, "Robust decentralized formation tracking control for stochastic large-scale biped robot team system under external disturbance and communication requirements," *IEEE Trans. Control. Netw. Syst.*, vol. 8, no. 2, pp. 654-666, Jun. 2021.

[30] S. Xu, T. Chen and J. Lam, "Robust H_∞ filtering for uncertain Markovian jump systems with mode-dependent time delays," *IEEE Trans. Automat. Contr.*, vol. 48, no. 5, pp. 900-907, May 2003.

[31] Z. Wang, F. Yang, D. W. C. Ho and X. Liu, "Robust H_∞ control for networked systems with random packet losses," *IEEE Trans. Syst., Man, Cybern. B*, vol. 37, no. 4, pp. 916-924, Aug. 2007.

[32] X. Lin, C. Wu and B. Chen, "Robust H_∞ Adaptive fuzzy tracking control for MIMO nonlinear stochastic poisson jump diffusion systems," *IEEE Trans. Cybern.*, vol. 49, no. 8, pp. 3116-3130, Aug. 2019.

[33] S. Ho, C. Chen and B. Chen, "Analysis for the robust H_∞ synchronization of nonlinear stochastic coupling networks through poisson processes and core coupling design," *IEEE Trans. Control. Netw. Syst.*, vol. 4, no. 2, pp. 223-235, Jun. 2017.

[34] P. Baranyi, "TP model transformation as a way to LMI-based controller design," *IEEE Trans. Ind. Electron*, vol. 51, no. 2, pp. 387-400, Apr. 2004.

[35] P. Baranyi, "The generalized TP model transformation for T–S fuzzy model manipulation and generalized stability verification," *IEEE Trans. Fuzzy Syst.*, vol. 22, no. 4, pp. 934-948, Aug. 2014.

[36] L. D. Lathauwer, B. D. Moor, and J. Vandewalle, "A multilinear singular value decomposition," *SIAM Journal on Matrix Analysis and Applications*, vol. 21, No. 4, pp. 1253–1278, Jan. 2000.

[37] P. Baranyi, P. Varlaki, L. Szeidl and Y. Yam, "Definition of the HOSVD based canonical form of polytopic dynamic models," in *Proc. 2006 IEEE Int. Conf. Mechatron.*, pp. 660-665.

[38] M. Yue, X. Hou, M. Fan and R. Jia, "Coordinated trajectory tracking control for an underactuated tractor-trailer vehicle via MPC and SMC approaches," in *Proc. 2017 2nd Int. Conf Adv. Robot. Mechatron. (ICARM)*, pp. 82-87.

[39] C. H. An, C. G. Atkeson, J. D. Griffiths and J. M. Hollerbach, "Experimental evaluation of feedforward and computed torque control," *IEEE Trans. Robot. Automat.*, vol. 5, no. 3, pp. 368-373, Jun. 1989.

[40] K. M. Lynch and F. C. Park, *Modern robotics: mechanics, planning,and control.* Cambridge, U. K.: Cambridge Univ. Press, 2017.

[41] J. Lee, H. Jung, H. Hu and D. H. Kim, "Collaborative control of UAV/UGV," in *Proc. 2014 11th Int. Conf. Ubiquitous Robot. Ambient Intell. (URAI)*, pp. 641-645.

[42] L. Chaimowicz, T. Sugar, V. Kumar and M. F. M. Campos, "An architecture for tightly coupled multi-robot cooperation," in *Proc. 2001 ICRA. IEEE Int. Conf. Robot. Autom.*, pp.2992-2997, vol.3.

[43] R. W. Beard, T. W. McLain, D. B. Nelson, D. Kingston and D. Johanson, "Decentralized cooperative aerial surveillance using fixed-wing miniature UAVs," *Proc. IEEE*, vol. 94, no. 7, pp. 1306-1324, July 2006.

[44] H. Park and S. A. Hutchinson, "Fault-tolerant rendezvous of multirobot systems," *IEEE Trans. Robot.*, vol. 33, no. 3, pp. 565-582, June 2017.

[45] S. Boyd, L. E. Ghaoui, E. Feron and V. Balakrishnan, *Linear matrix inequalities in system and control theory.* Philadelphia, PA, USA: SIAM, 1994.

[46] C. S. Tseng, B. S. Chen and H. J. Uang, "Fuzzy tracking control design for nonlinear dynamic systems via T-S fuzzy model," *IEEE Trans. Fuzzy Syst.*, vol. 9, no. 3, pp. 381-392, June 2001.

[47] G. Feng, "A survey on analysis and design of model-based fuzzy control systems," *IEEE Trans. Fuzzy Syst.*, vol. 14, no. 5, pp. 676-697, Oct. 2006.

[48] O. Michel, "Webots: professional mobile robot simulation," *Int. J. Adv. Robot. Syst.*, vol. 1, no. 1, pp. 39-42, Mar. 2004.

[49] Y. Chang and B. Chen, "A fuzzy approach for robust reference-tracking-control design of nonlinear distributed parameter time-delayed systems and its application," *IEEE Trans. Fuzzy Syst.*, vol. 18, no. 6, pp. 1041-1057, Dec. 2010.

[50] W. Zhang, L. Xie and B. S. Chen, *Stochastic H_2/H_∞ control: A Nash Game Approach*. Boca Raton, FL, USA: CRC Press, 2017.

[51] A. J. van der Schaft, "L/sub 2/-gain analysis of nonlinear systems and nonlinear state-feedback H/sub infinity / control," *IEEE Trans. Automat. Contr.*, vol. 37, no. 6, pp. 770-784, June 1992.